To appear in IEEE Transactions on Power Systems
Vol. 1, No. 2, May 2003

Computing Small-Signal Stability Boundaries for Large-Scale Power Systems

Sergio Gomes Jr., CEPEL
Nelson Martins, CEPEL
Carlos Portela, COPPE/UFRJ

Rio de Janeiro - Brazil

Acknowledgements

- Herminio Pinto, previously with CEPEL
- Paulo Eduardo M. Quintão, FPLF-PUC/RJ
- Alex de Castro, FPLF-PUC/RJ

System Equations Linearized at Singular Point X_0

$$\mathbf{T} \cdot \dot{\mathbf{x}} = \mathbf{f}(\mathbf{x}, u)$$
$$y \quad = \mathbf{h}(\mathbf{x}, u)$$

$$\mathbf{f}(\mathbf{x_0}) = \mathbf{0}$$

$$\mathbf{T} \cdot \Delta\dot{\mathbf{x}} = \mathbf{J} \cdot \Delta\mathbf{x} + \mathbf{b} \cdot \Delta u$$
$$\Delta y \quad = \mathbf{c} \cdot \Delta\mathbf{x} + d \cdot \Delta u$$

Basic Equations for the Hopf Algorithm

$$\left[\lambda^{spec}\cdot\mathbf{T}-\mathbf{J}(p)\right]\cdot\mathbf{v}=\mathbf{0}$$

$$\mathbf{c}\cdot\mathrm{v}=1$$

- λ^{spec} is the specified value for a complex pole, to be reached through an appropriate change to the system parameter "*p*"
- The second equation defines the norm of the eigenvector "**v**"
- Solution by Newton-Raphson

Small-Signal Stability and Security Boundaries

$$B(\sigma, \omega) = 0$$

Where

$$B(\sigma, \omega) = \sigma + \frac{\zeta}{\sqrt{1-\zeta^2}} \cdot \omega$$

$$\lambda = \sigma \pm j\omega$$

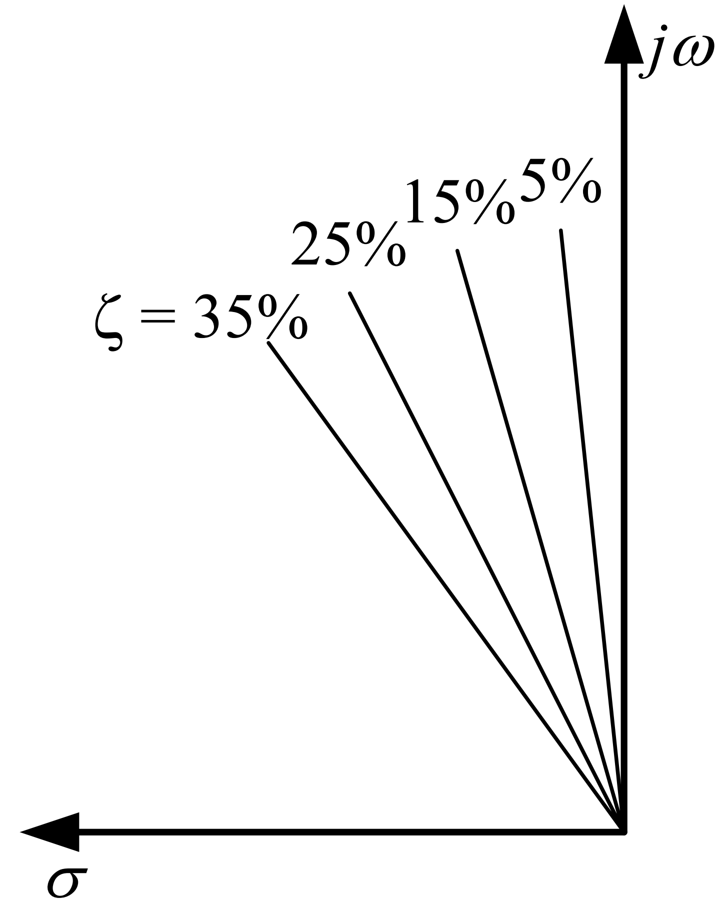

Non-Linear Equations for Security Boundary (Modified Hopf) Algorithm

$$\mathbf{f}\left(\mathbf{x_0}, p\right) = 0$$

$$\left[\lambda \cdot \mathbf{T} - \mathbf{J}\left(\mathbf{x_0}, p\right)\right] \cdot \mathbf{v} = \mathbf{0}$$

$$\mathbf{c} \cdot \mathbf{v} = 1$$

$$B\left(\sigma, \omega\right) = 0$$

Matrix Problem to be Solved at Every Iteration

$$\left[\begin{array}{c:c:c:c:c} \sigma \cdot \mathbf{T} - \mathbf{J} & -\omega \cdot \mathbf{T} & \mathbf{T} \cdot \mathbf{v}_{\mathbf{re}} & -\mathbf{T} \cdot \mathbf{v}_{\mathbf{im}} & -\dfrac{\partial \mathbf{J}}{\partial p}\mathbf{v}_{\mathbf{re}} \\ \hdashline \omega \cdot \mathbf{T} & \sigma \cdot \mathbf{T} - \mathbf{J} & \mathbf{T} \cdot \mathbf{v}_{\mathbf{im}} & \mathbf{T} \cdot \mathbf{v}_{\mathbf{re}} & -\dfrac{\partial \mathbf{J}}{\partial p}\mathbf{v}_{\mathbf{im}} \\ \hdashline \mathbf{c} & & & & \\ \hdashline & \mathbf{c} & & & \\ \hdashline & & \dfrac{\partial B}{\partial \sigma} & \dfrac{\partial B}{\partial \omega} & \end{array}\right] \cdot \left[\begin{array}{c} \mathbf{v}_{\mathbf{re}}^{\mathbf{new}} \\ \hdashline \mathbf{v}_{\mathbf{im}}^{\mathbf{new}} \\ \hdashline \Delta\sigma \\ \hdashline \Delta\omega \\ \hdashline \Delta p \end{array}\right] = \left[\begin{array}{c} \mathbf{0} \\ \hdashline \mathbf{0} \\ \hdashline 1 \\ \hdashline 0 \\ \hdashline -B \end{array}\right]$$

Compact Form for Hopf Equations Involving the Prior Factorization of the System Jacobian Equations

$$\begin{bmatrix} \Re[\mathbf{c}\cdot\mathbf{v}_1] & -\Im[\mathbf{c}\cdot\mathbf{v}_1] & \Re[\mathbf{c}\cdot\mathbf{v}_2] \\ \Im[\mathbf{c}\cdot\mathbf{v}_1] & \Re[\mathbf{c}\cdot\mathbf{v}_1] & \Im[\mathbf{c}\cdot\mathbf{v}_2] \\ \dfrac{\partial B}{\partial \sigma} & \dfrac{\partial B}{\partial \omega} & 0 \end{bmatrix} \cdot \begin{bmatrix} \Delta\sigma \\ \Delta\omega \\ \Delta p \end{bmatrix} = \begin{bmatrix} 1 \\ 0 \\ -B \end{bmatrix}$$

Hopf Bifurcations

- Compute parameter values that cause critical eigenvalues to cross small-signal stability boundary
- Hopf bifurcations are computed for:
  - Single-parameter changes
  - Multiple-parameter changes (minimum distance in the parameter space)

Experience with Inter-Area Oscillation Problems (1/2)

Michigan-Ontario-Quebec	1959
Saskatchewan-Manitoba-Ontario West	1962-1965
Western USA (WSCC)	1964-1978
Sweden-Finland-Norway-Denmark	Late 1960's
Mid-continent Area Power Pool (MAPP)	1971-1970
Italy-Yugoslavia-Austria	1971-1974
South East Australia	1975
Scotland-England	1978
Western Australia	1982-1983
Taiwan	1984

Experience with Inter-Area Oscillation Problems (2/2)

Ghana-Ivory Coast	1985
Southern Brazil	1985-1987
Ontario Hydro	1985
Brazilian North-Northeast	1986
Venezuela-Colombia Interconnection	1992
Argentinean Interconnected System (SADI)	1998
South-African Cone	1998
Brazilian North-South	2000

Original slide from Dr. Prabha Kundur, with the last five additions by the authors

North-Northeast Interconnection (1988)

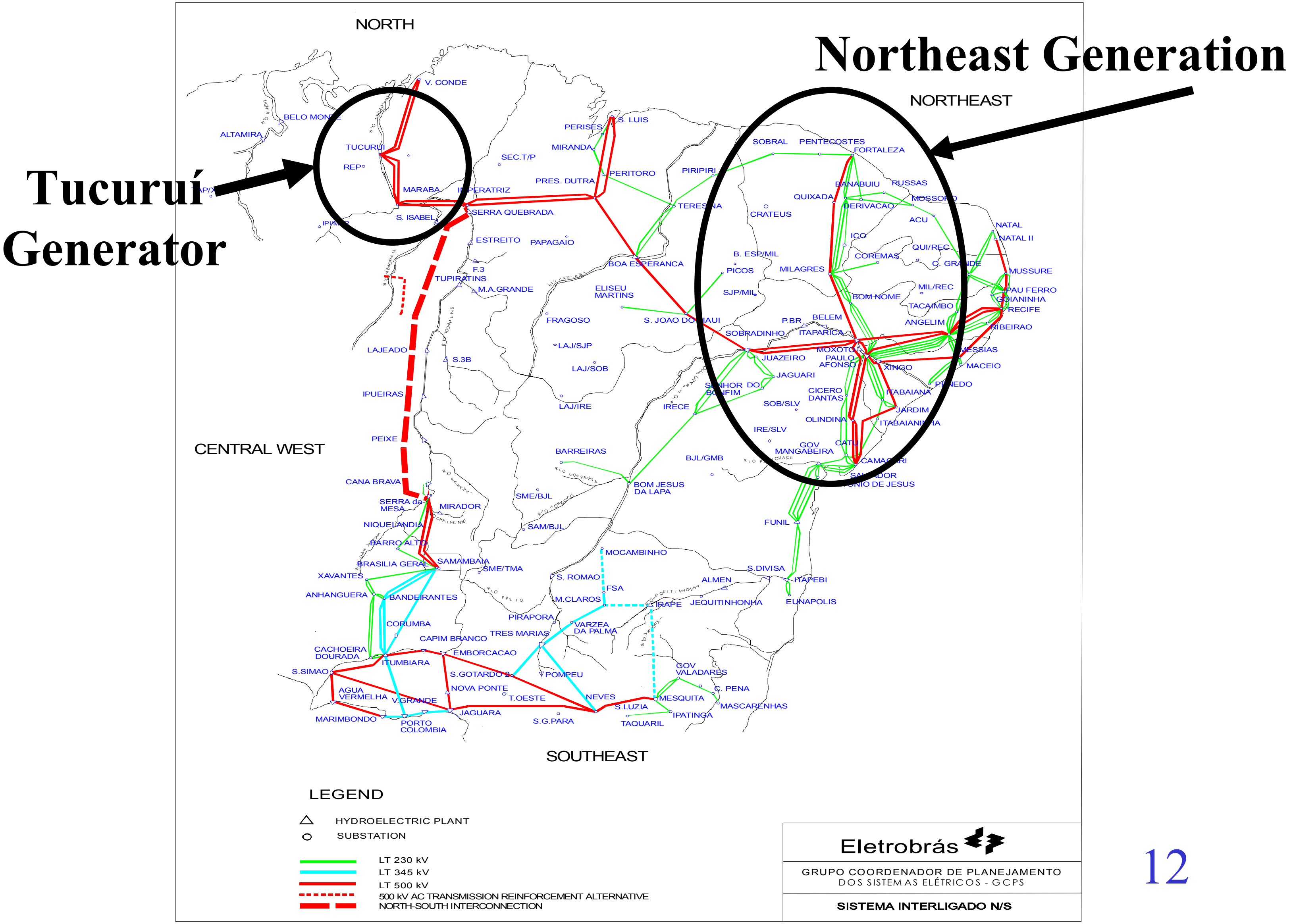

Brazilian N/NE Interconnection

Spontaneous oscillations controlled by operator through MW reduction

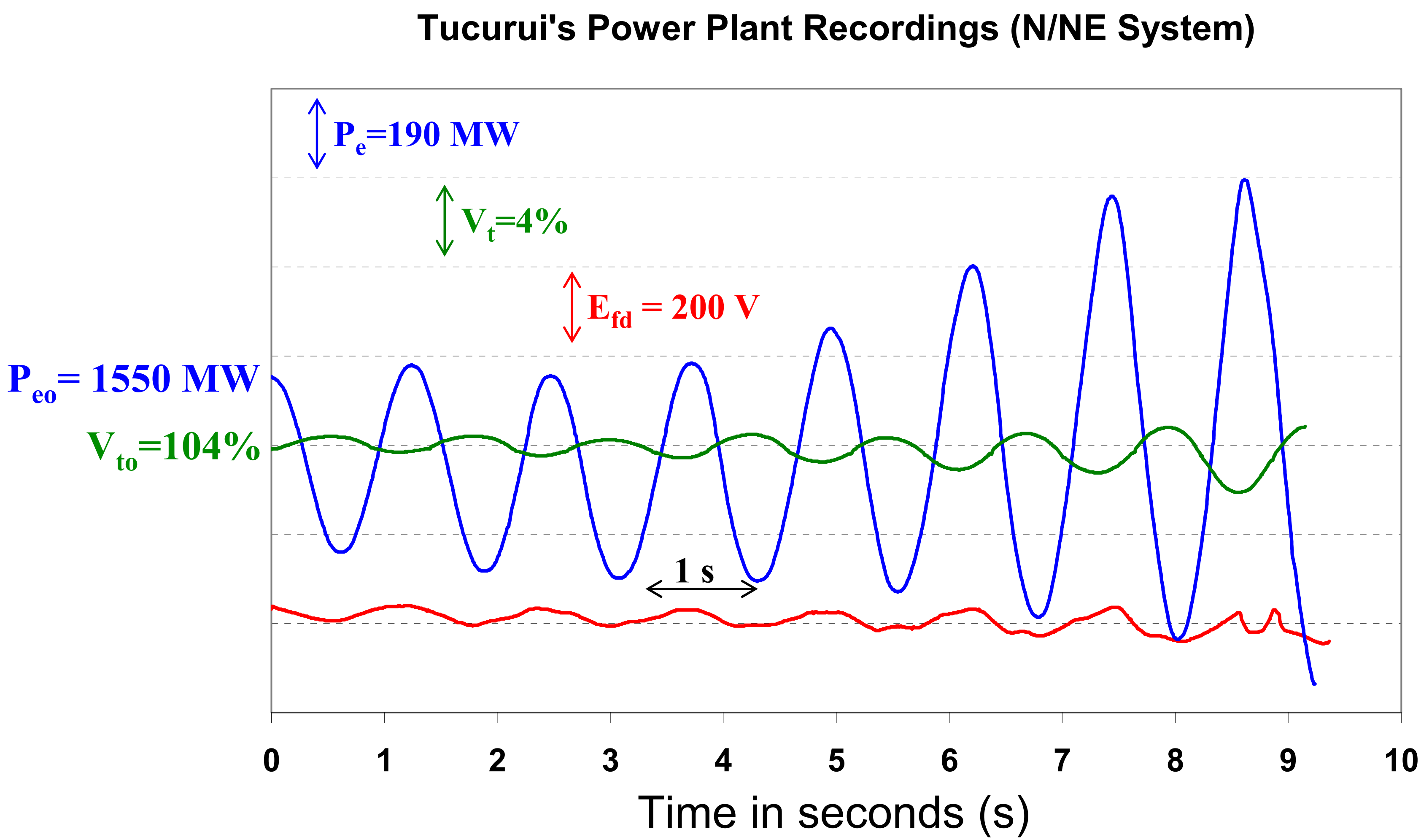

Oscillation problem later solved via PSS retuning

Section 7.9 of CIGRE TF 38.02.16 Document
“Impact of the Interaction Among P. System Controls”

Field Tests to Determine the Effectiveness of the TCSC Controllers in Damping the Brazilian North-South Intertie Oscillations

C. Gama — Eletronorte
L. Ängquist, G. Ingeström, M. Noroozian — ABB

The North-South Brazilian Interconnection

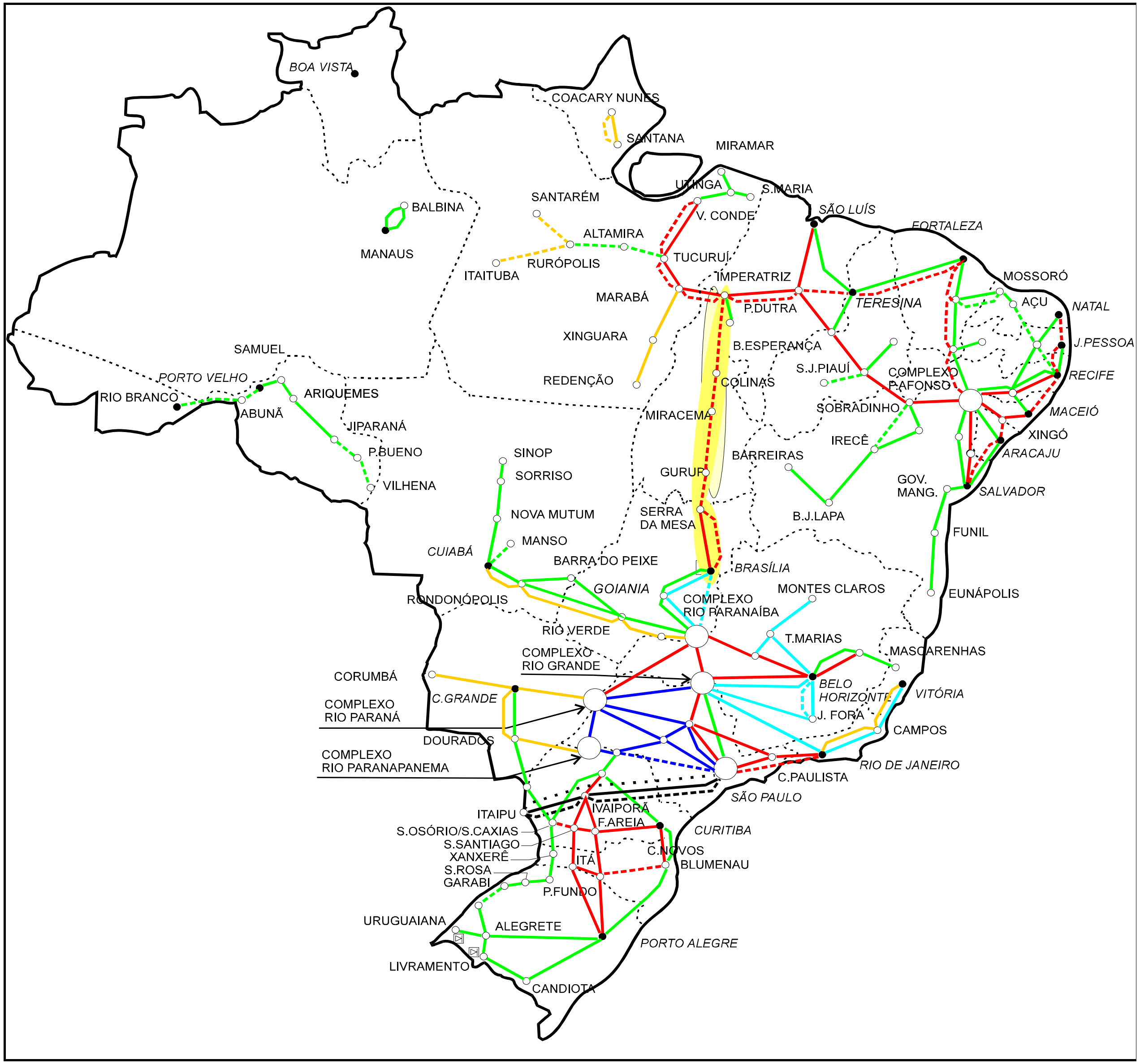

TCSCs Located at the Two Ends of the North-South Intertie

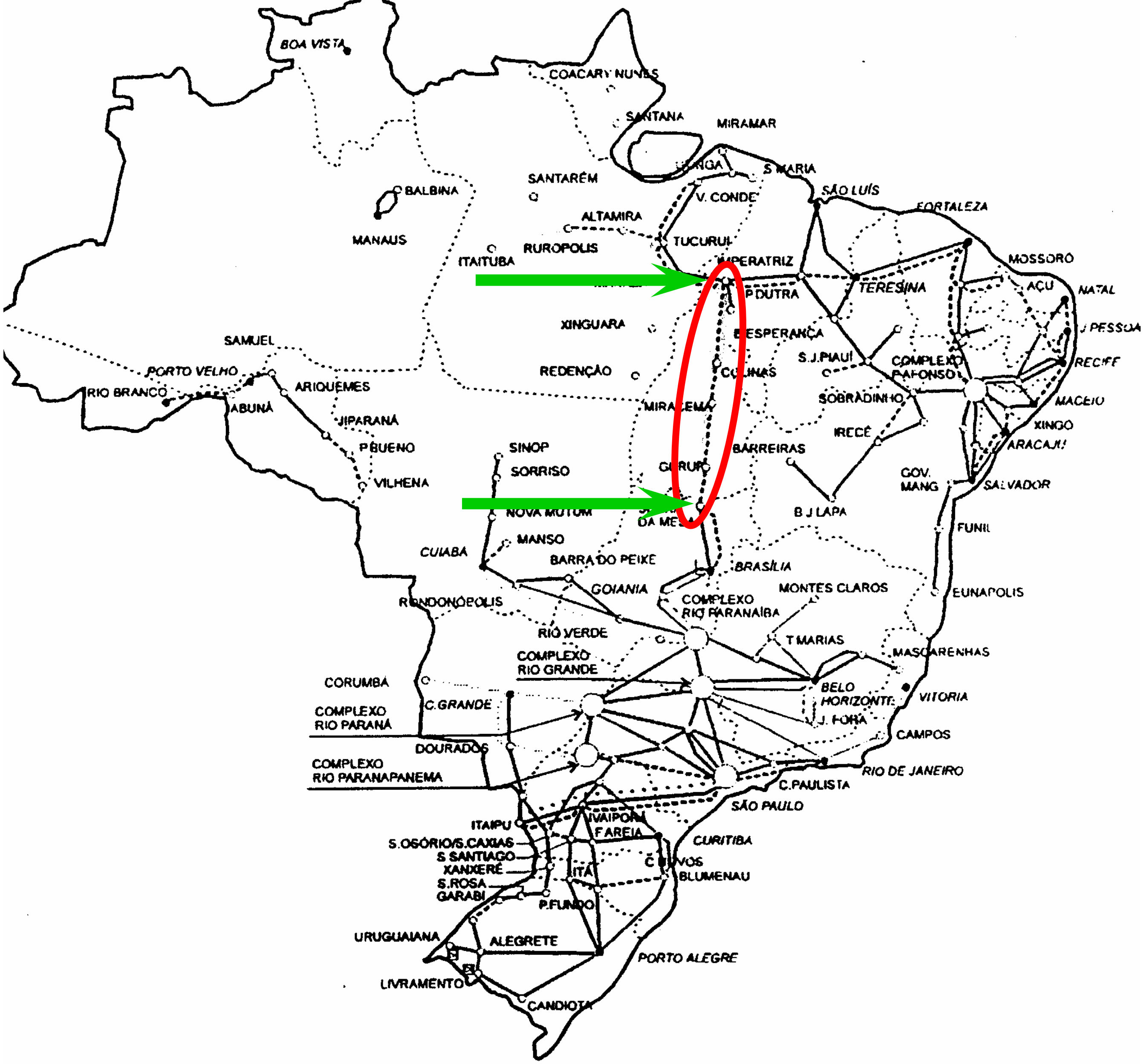

System Staged Tests – no PODs on 2 TCSCs

Brazilian North-South System goes Unstable!

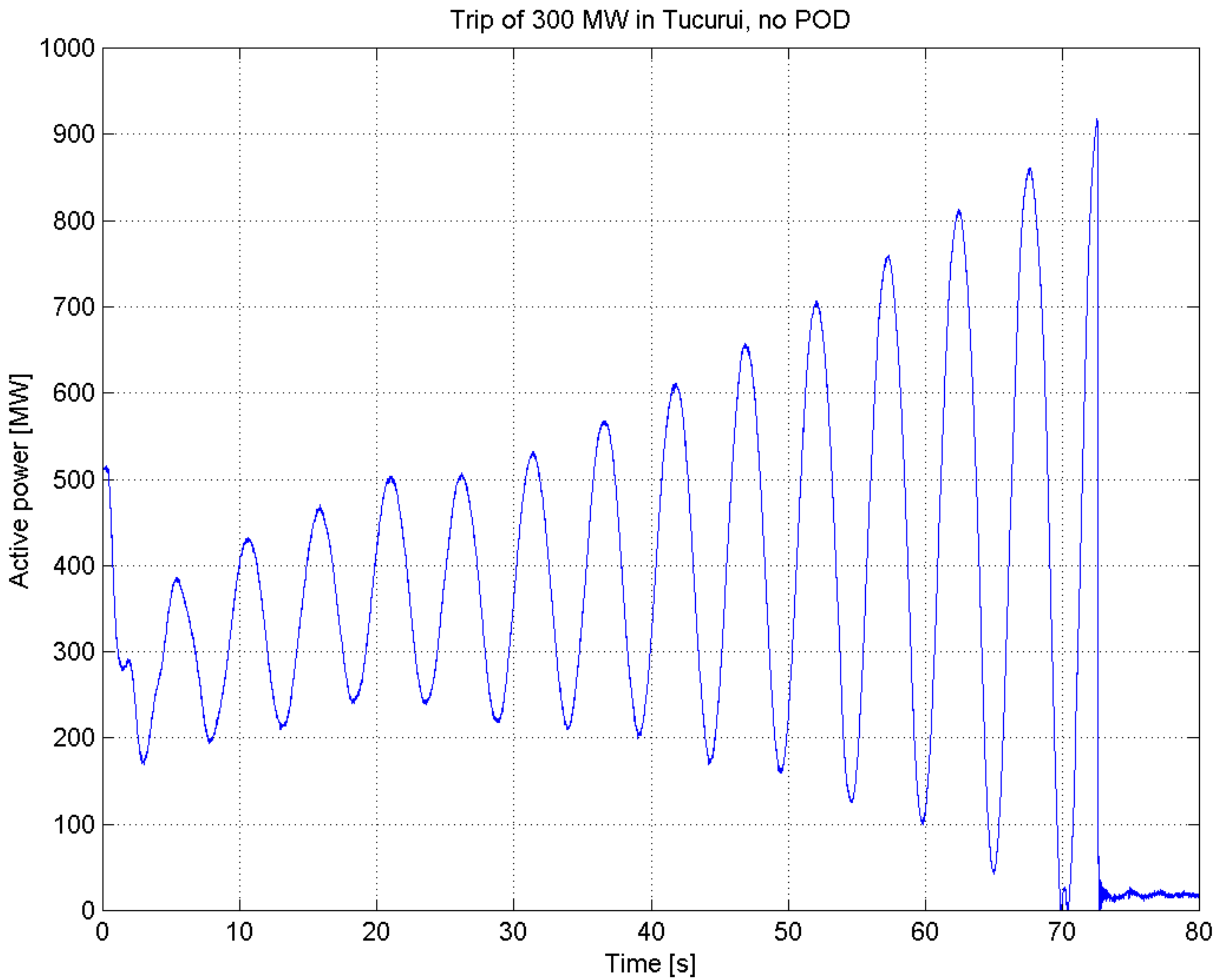

System Staged Tests – with 2 PODs

Brazilian North-South System is now stable

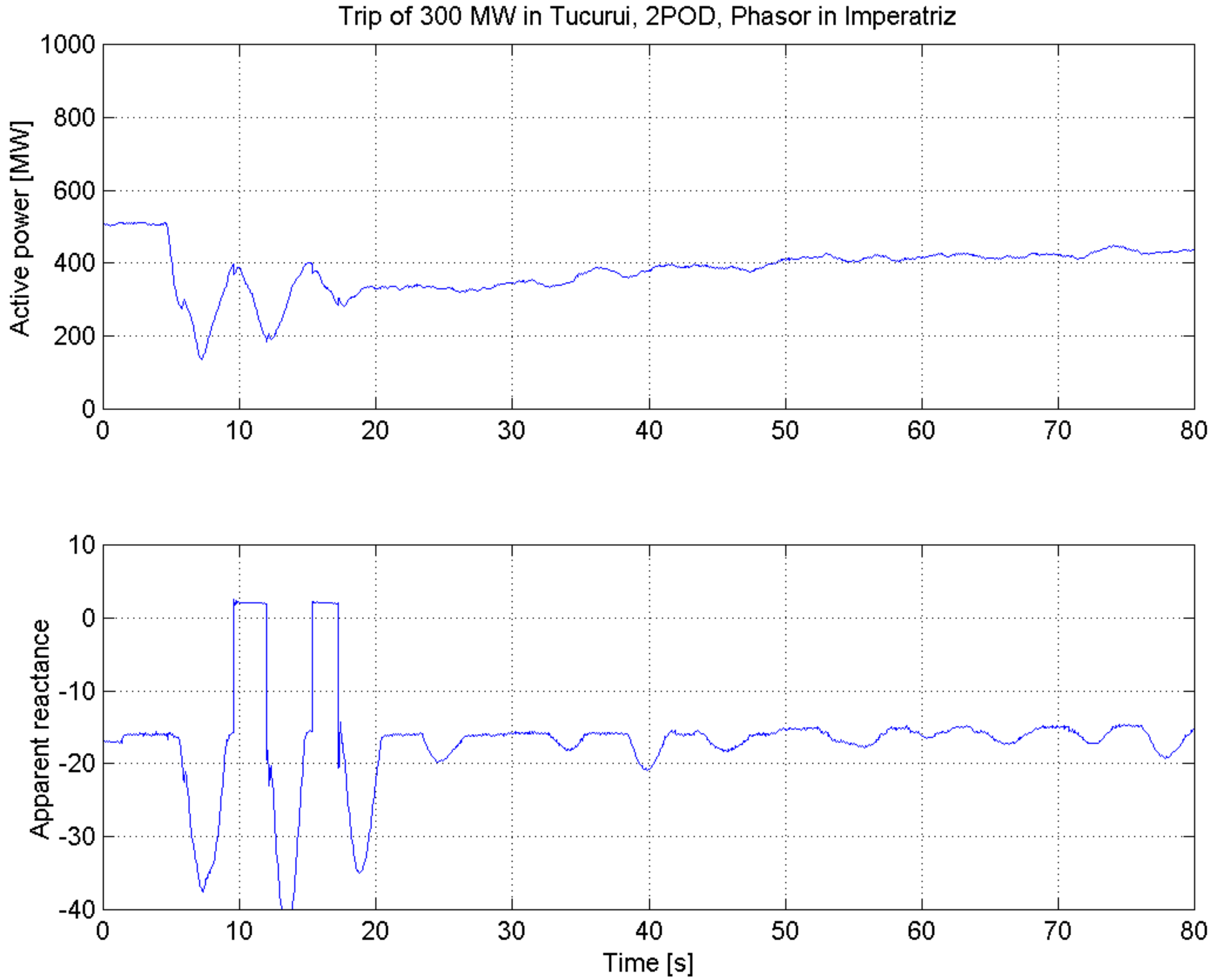

Large-Scale, Decentralized Oscillation Damping Control Problem

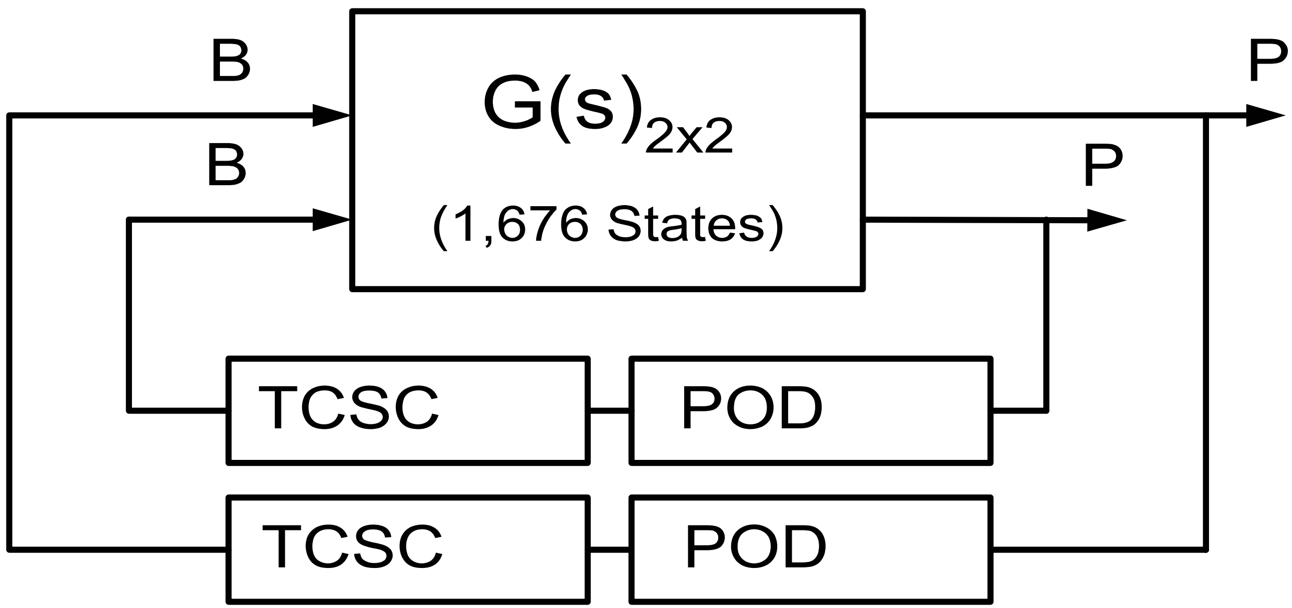

Hopf Bifurcations – Test System Utilized

- System Data:
  - 2400 buses, 3400 lines/transformers, 2520 loads
  - 120 generators, 120 AVRs, 46 PSSs, 100 speed-governors
  - 1 HVDC link (6,000 MW)
  - 4 SVCs
  - 2 TCSCs

- Jacobian Matrix:
  - 13.062 lines
  - 48.521 non-zeros
  - 1676 states

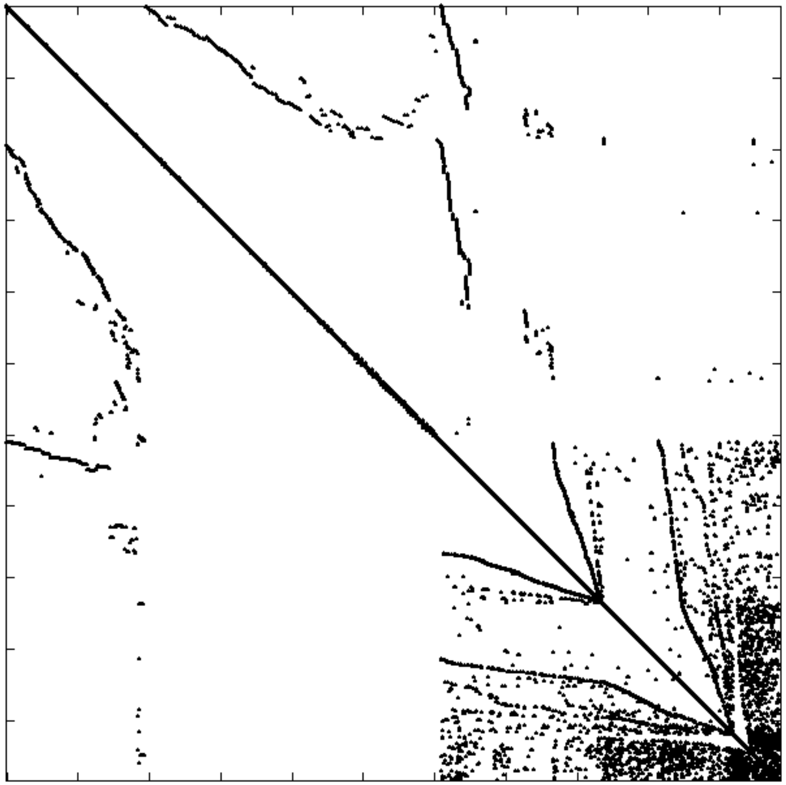

Hopf Bifurcations – Test System Problem

- The TCSCs are located one at each end of the North-South intertie and are equipped with PODs to damp the 0.17 Hz mode

- The Hopf bifurcation algorithms were applied to compute eigenvalue crossings of the security boundary (5% damping ratio) for simultaneous gain changes in the two PODs

Eigenvalue (Pole) Spectrum for Brazilian North-South System (1,676 eigenvalues)

Poles in window near the origin are shown enlarged in next slides

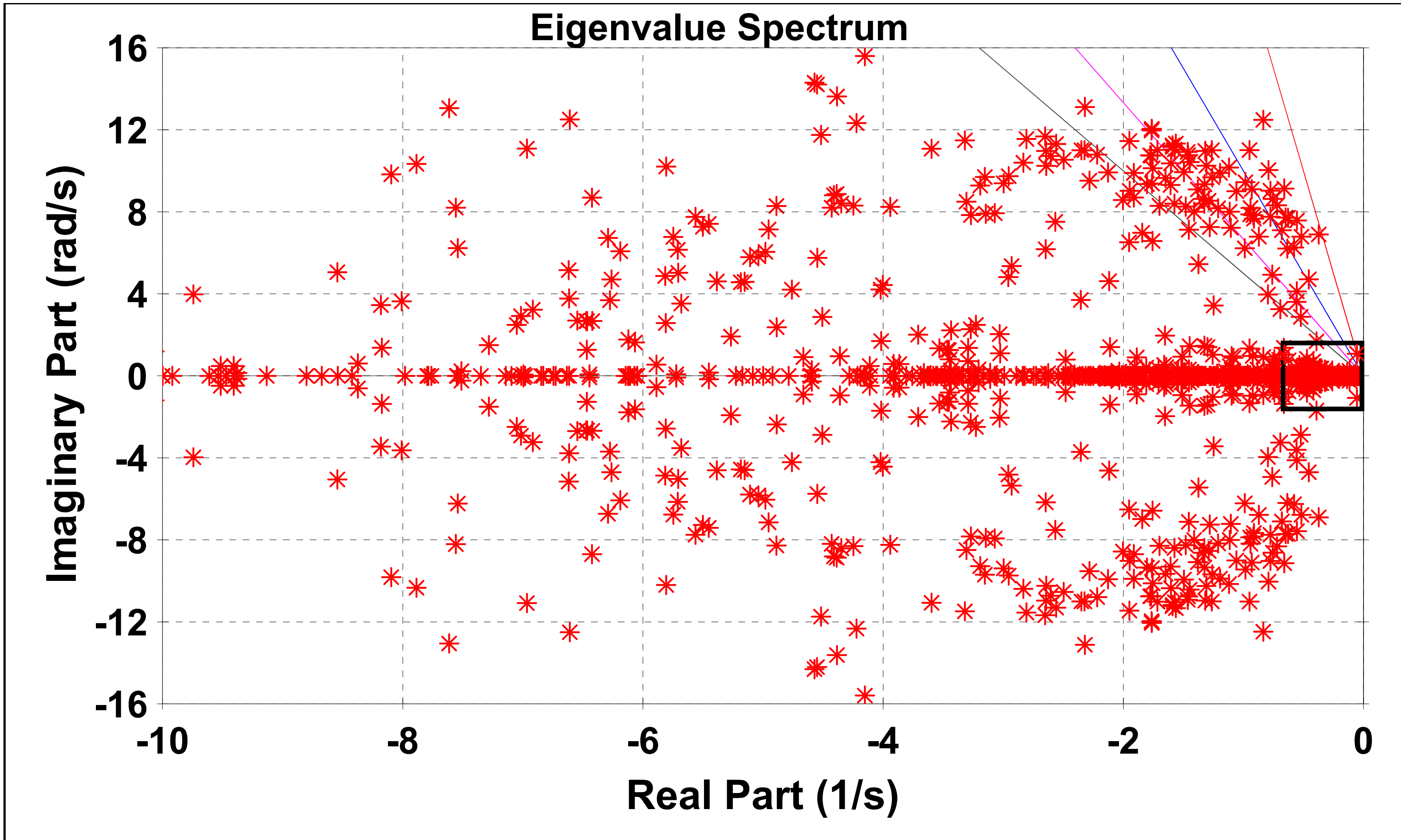

Root Locus (focusing on the critical poles within small window) when Reducing the Gains of the 2 TCSCs

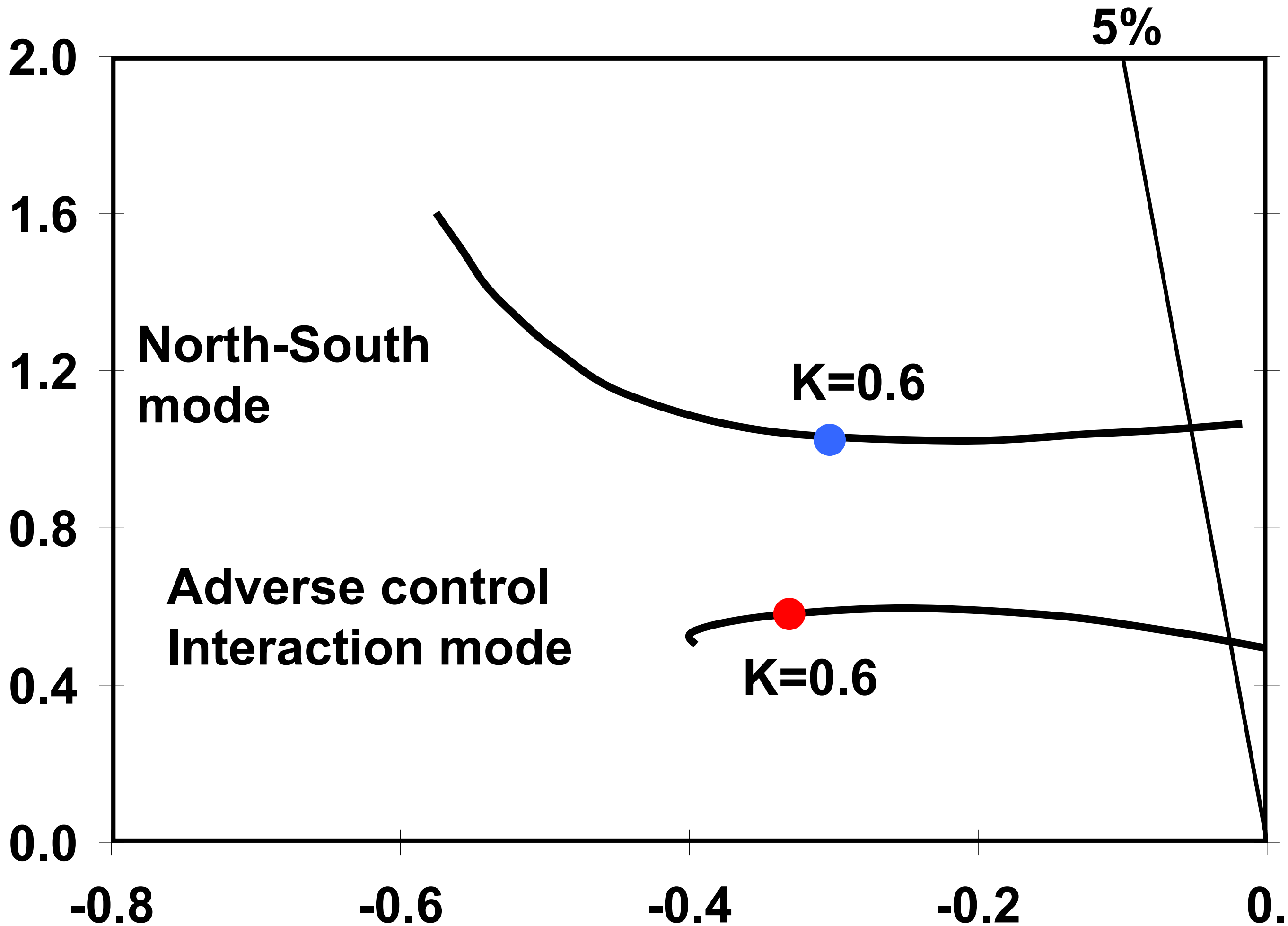

Root Locus (focusing on the critical poles within small window) when Reducing the Gains of the 2 TCSCs

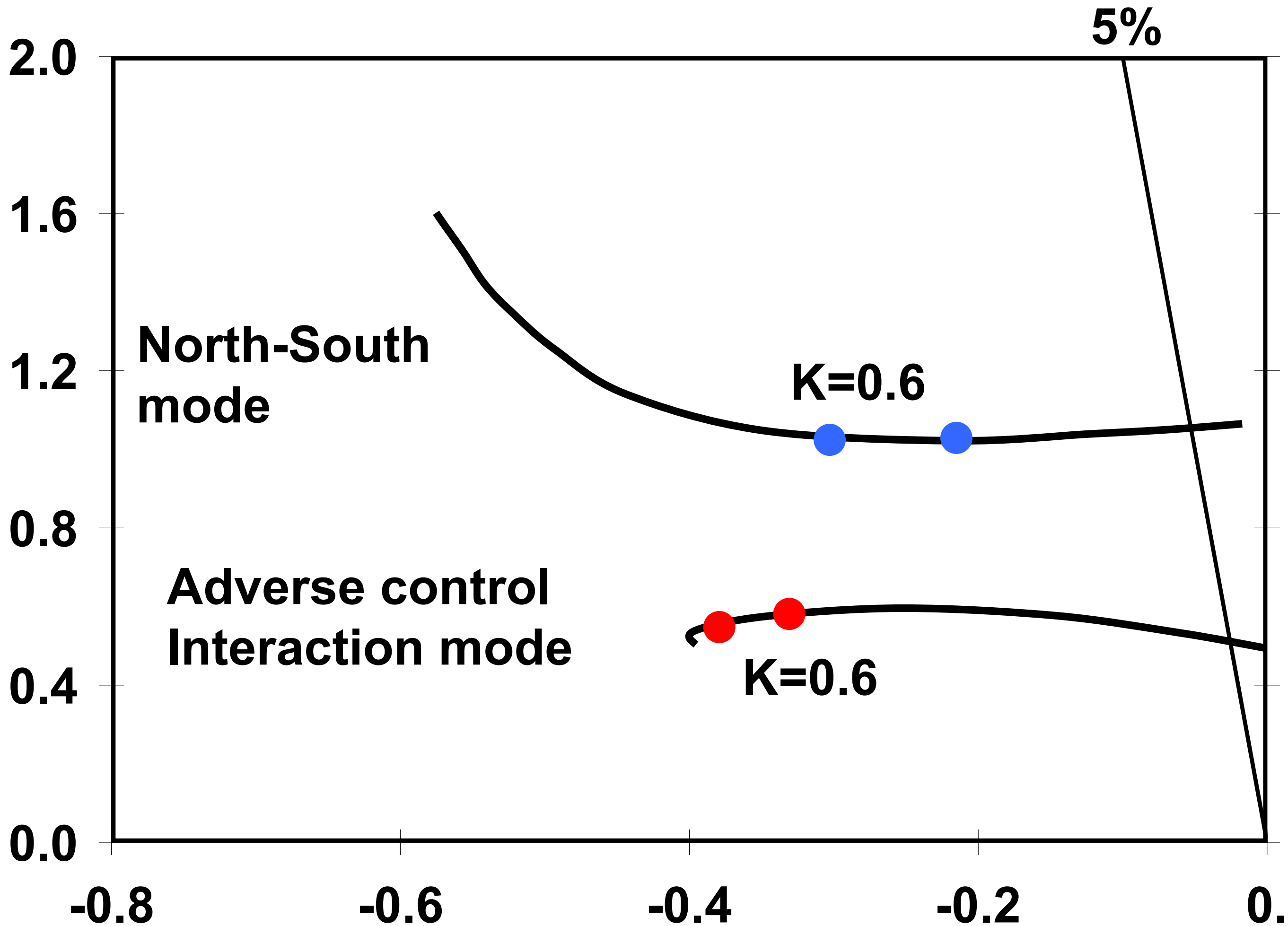

Root Locus (focusing on the critical poles within small window) when Reducing the Gains of the 2 TCSCs

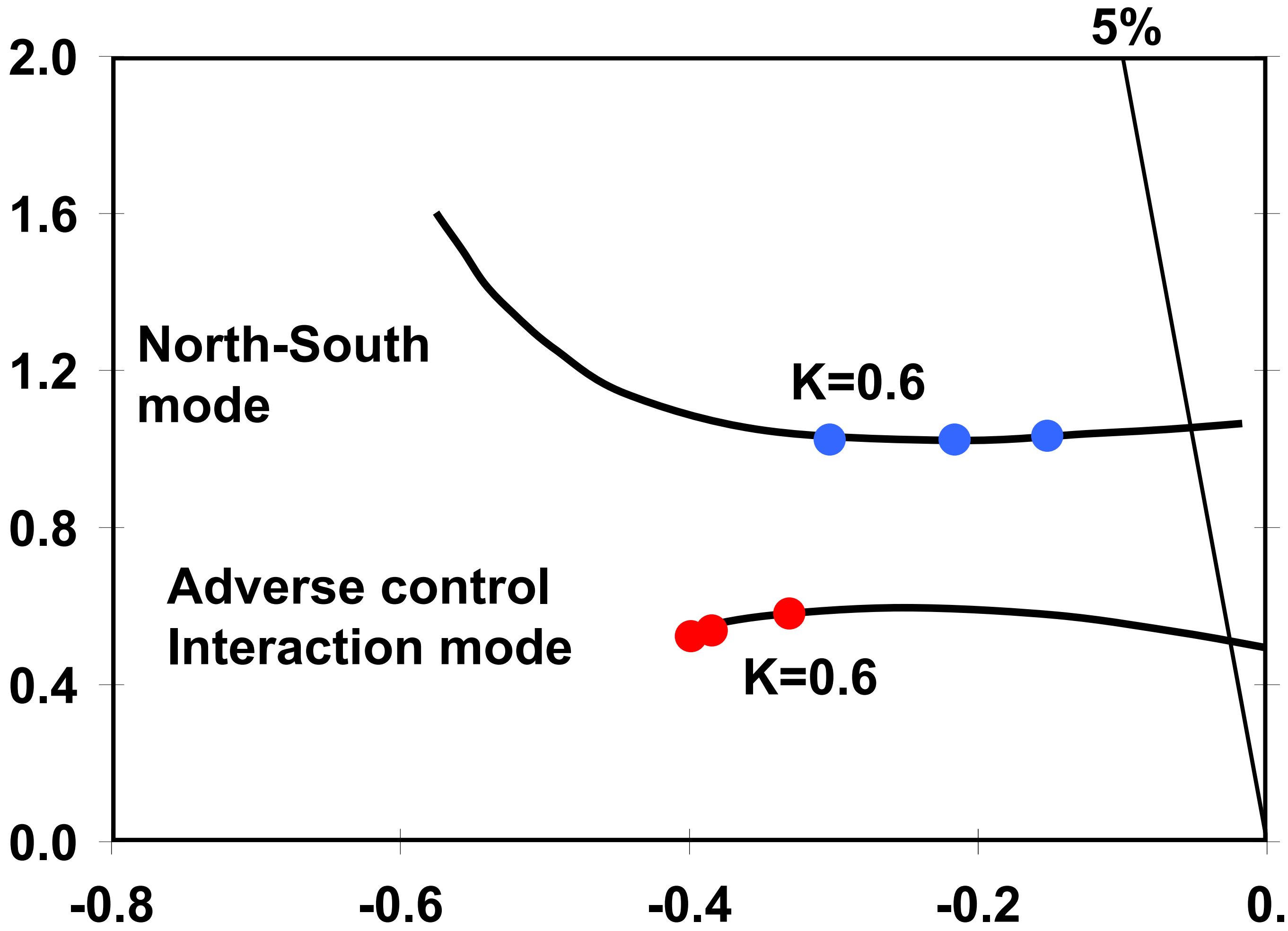

Root Locus (focusing on the critical poles within small window) when Reducing the Gains of the 2 TCSCs

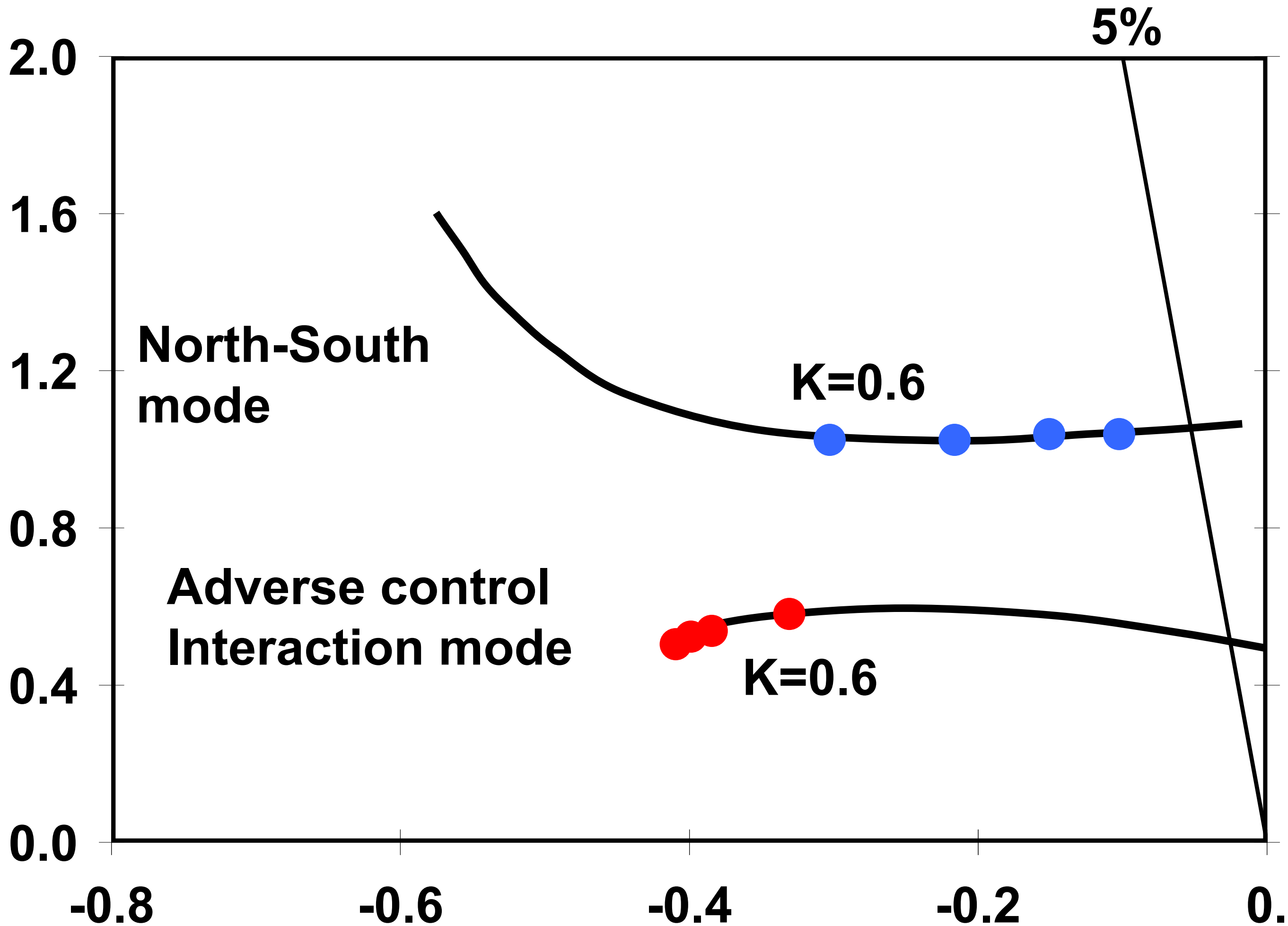

Root Locus (focusing on the critical poles within small window) when Reducing the Gains of the 2 TCSCs

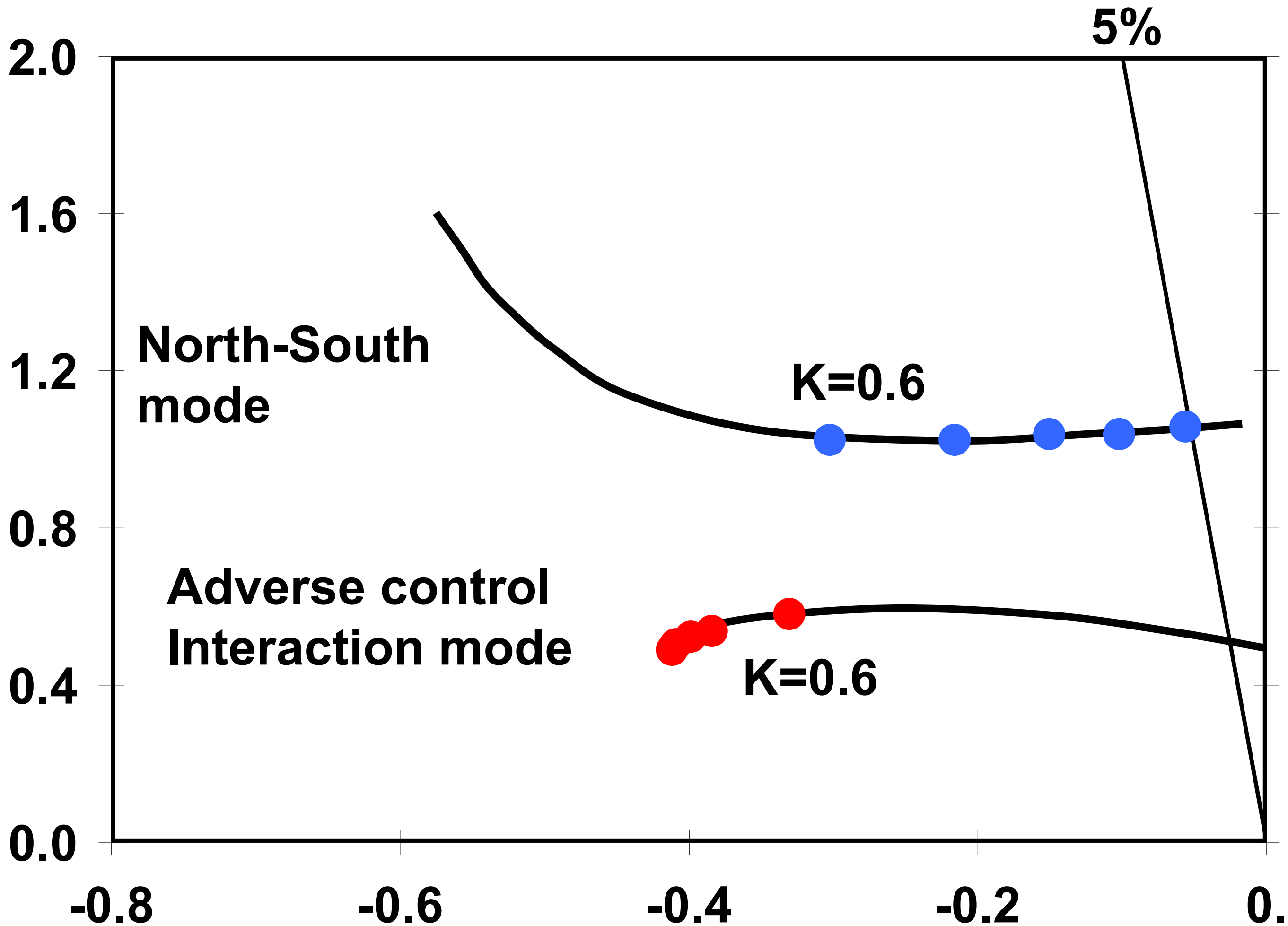

Root Locus (focusing on the critical poles within small window) when Reducing the Gains of the 2 TCSCs

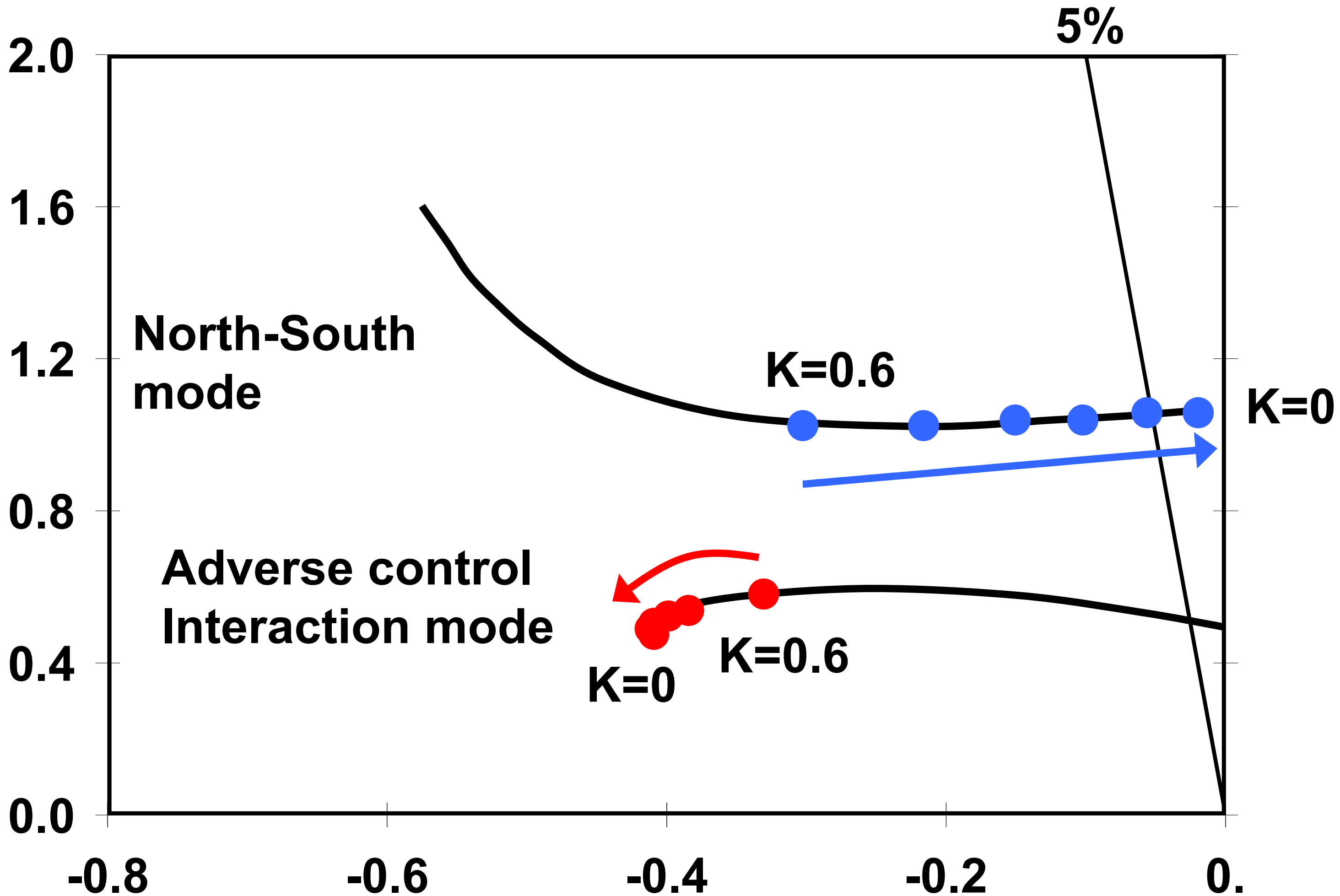

Root Locus (focusing on the critical poles within small window) when Increasing the Gains of the 2 TCSCs

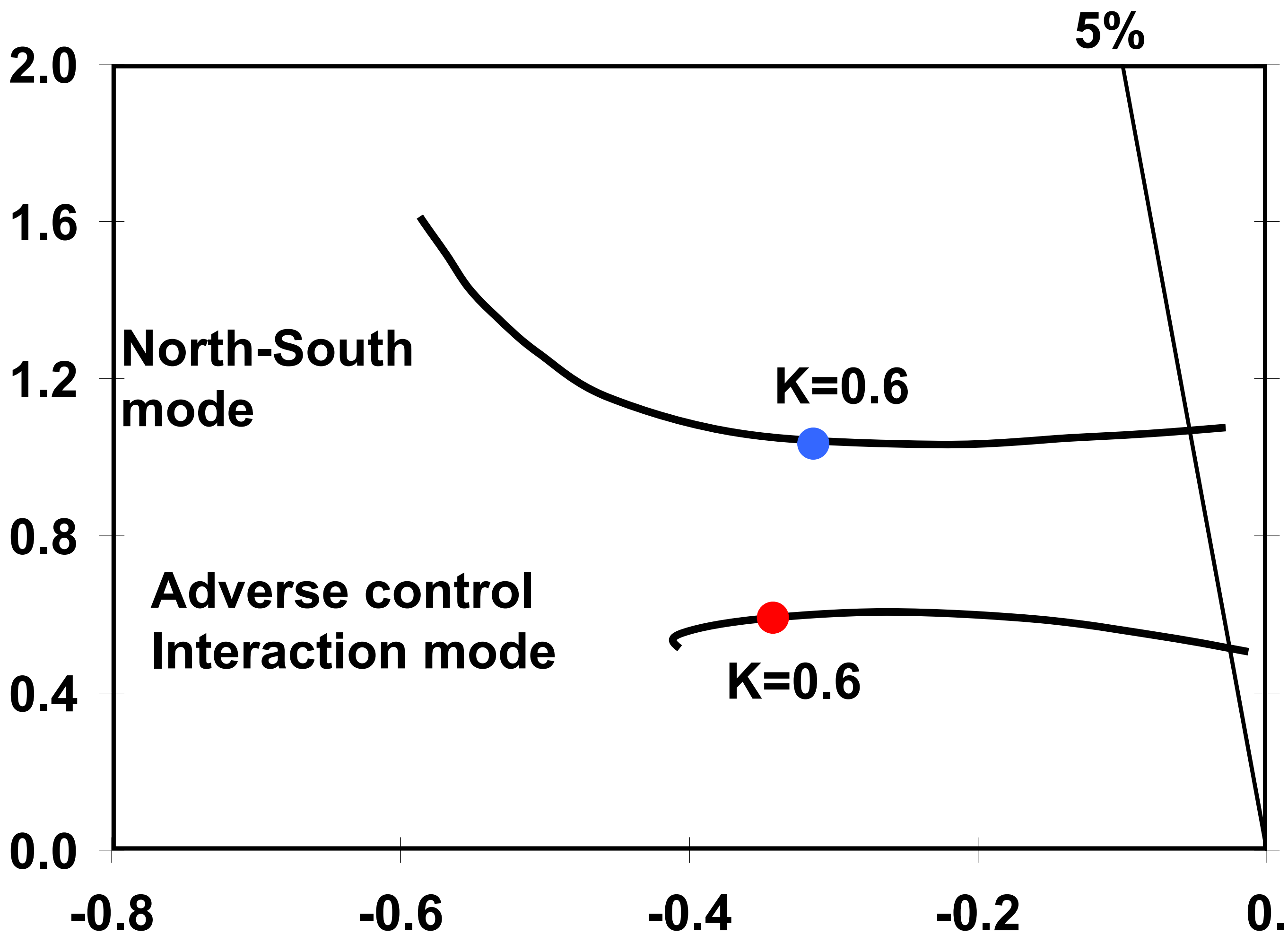

Root Locus (focusing on the critical poles within small window) when Increasing the Gains of the 2 TCSCs

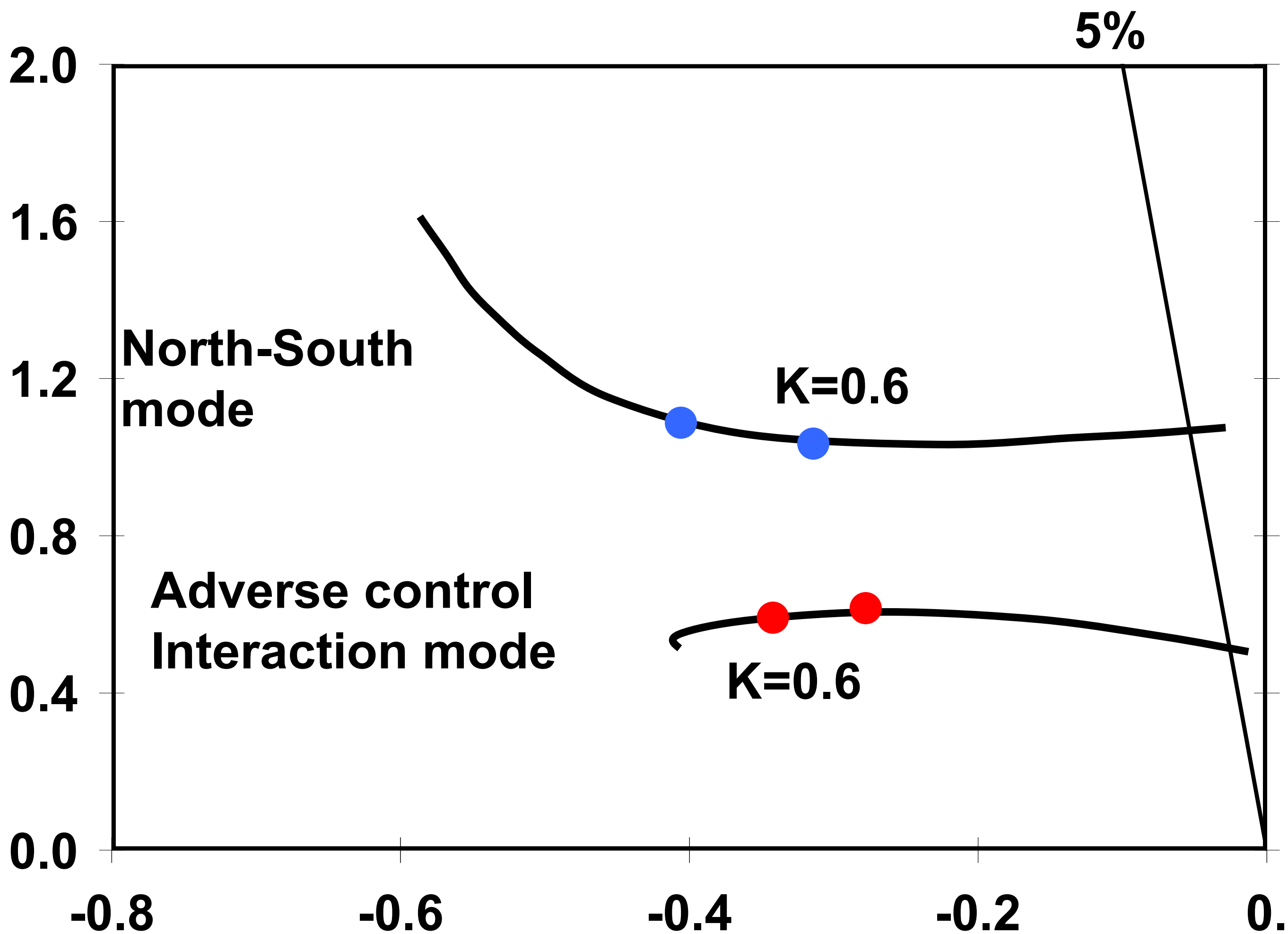

Root Locus (focusing on the critical poles within small window) when Increasing the Gains of the 2 TCSCs

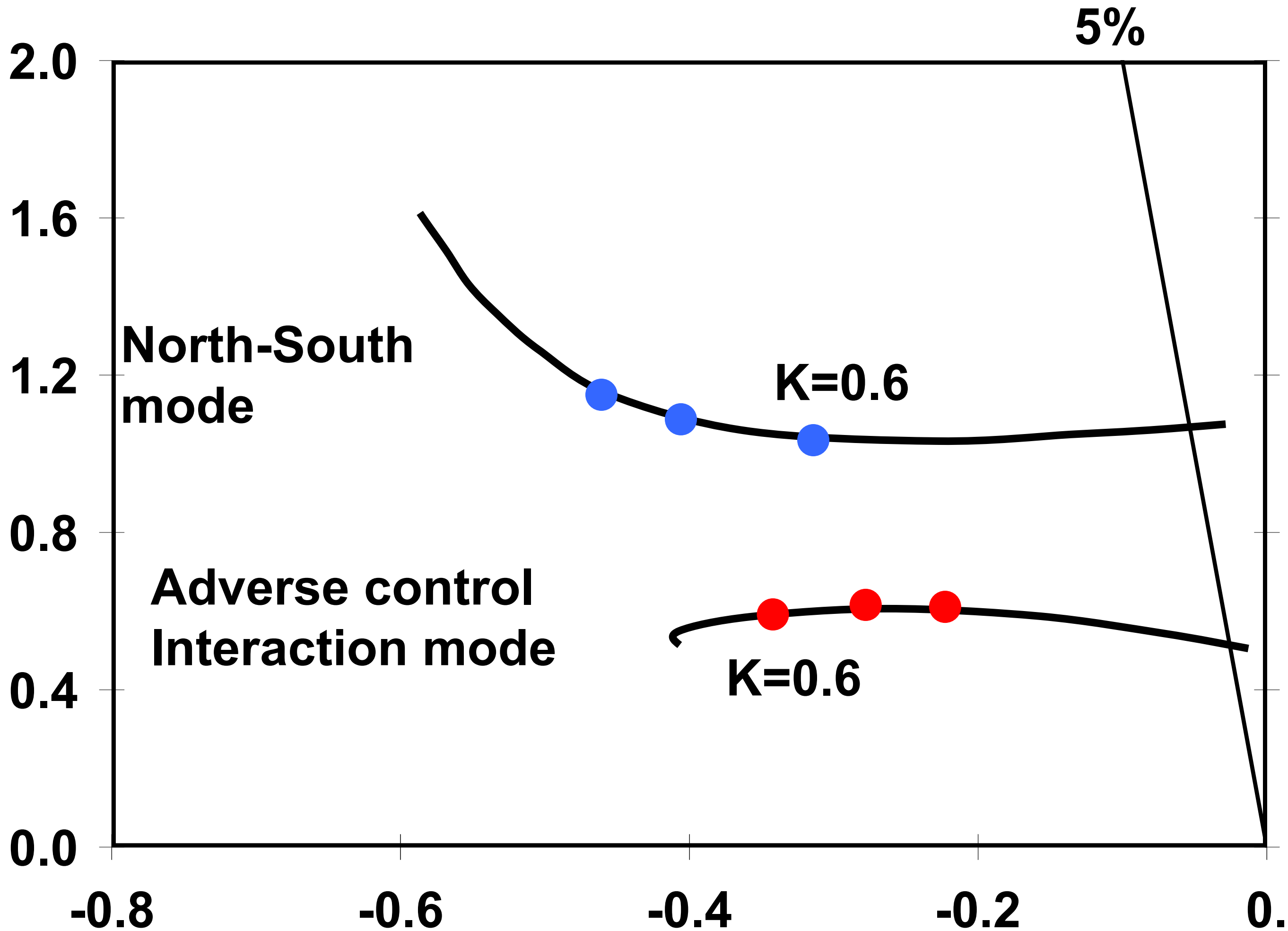

Root Locus (focusing on the critical poles within small window) when Increasing the Gains of the 2 TCSCs

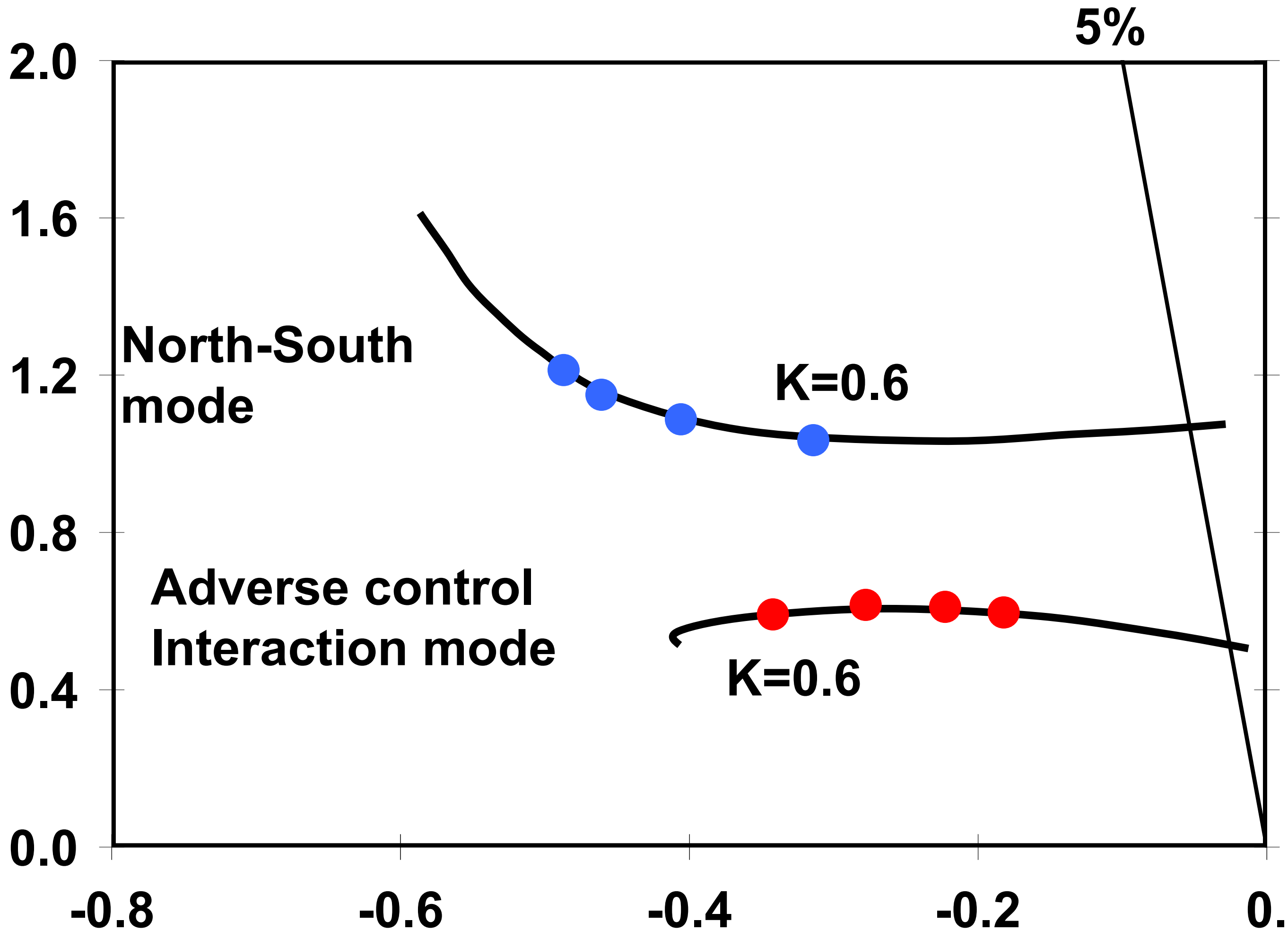

Root Locus (focusing on the critical poles within small window) when Increasing the Gains of the 2 TCSCs

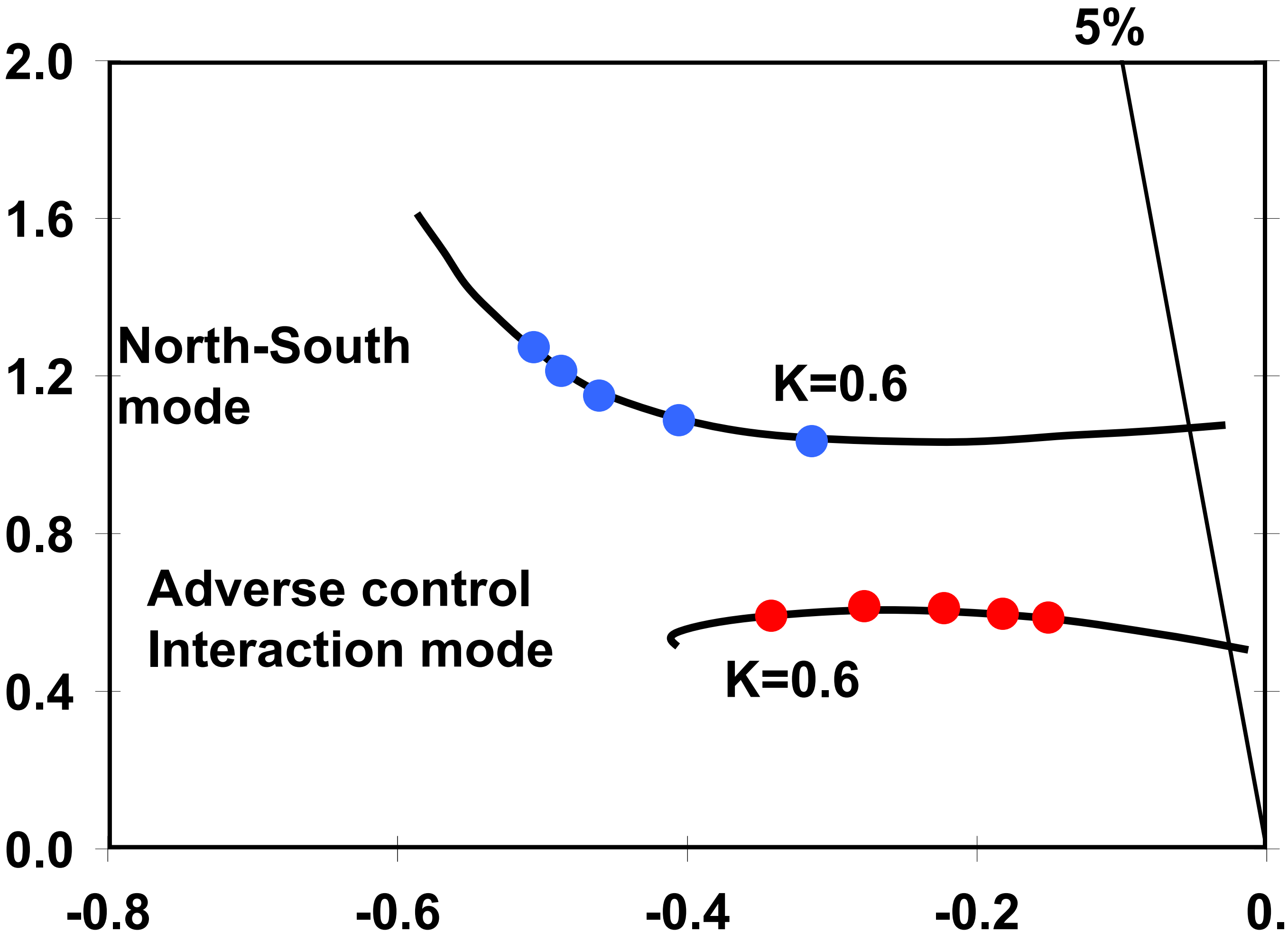

Root Locus (focusing on the critical poles within small window) when Increasing the Gains of the 2 TCSCs

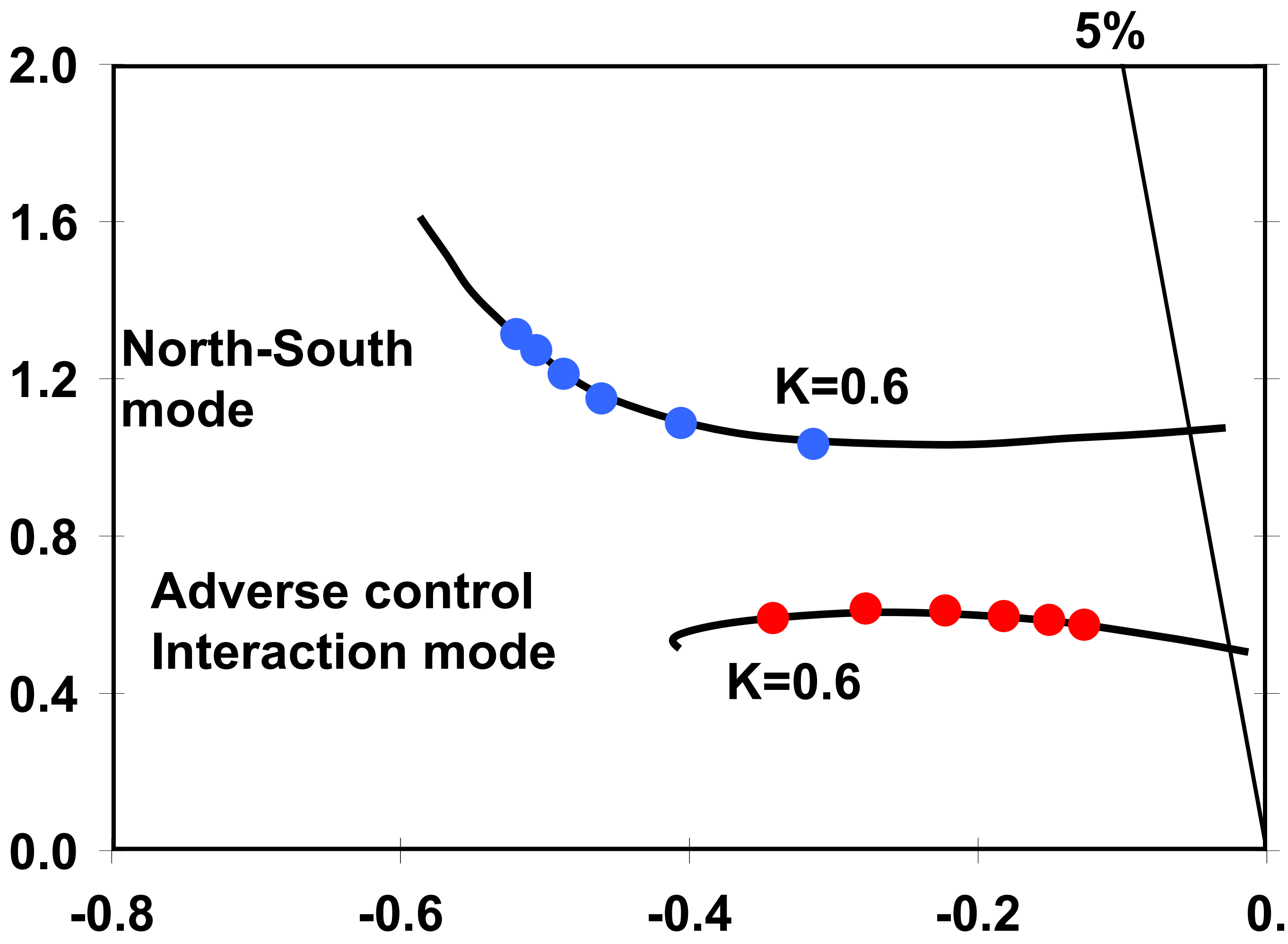

Root Locus (focusing on the critical poles within small window) when Increasing the Gains of the 2 TCSCs

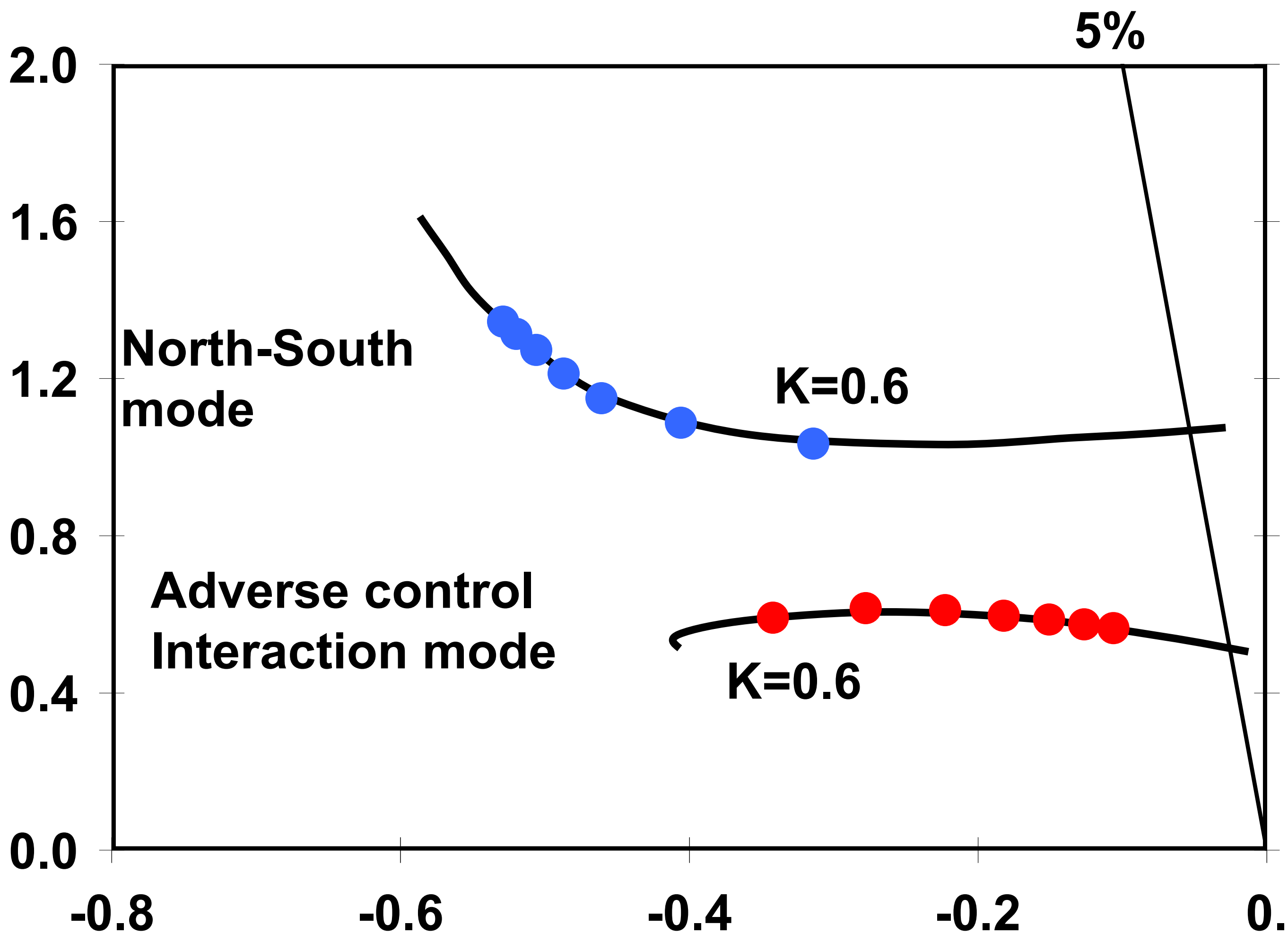

Root Locus (focusing on the critical poles within small window) when Increasing the Gains of the 2 TCSCs

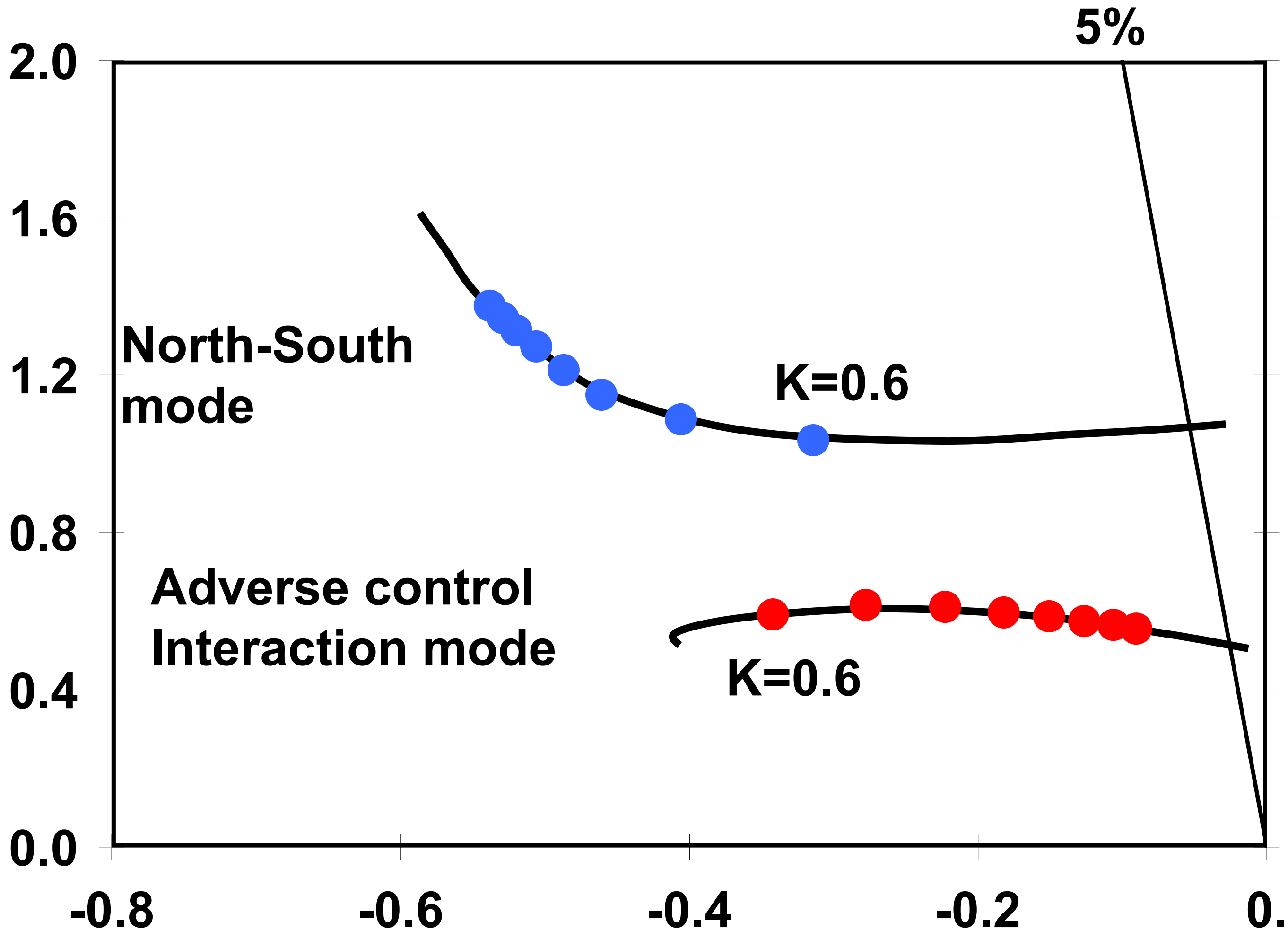

Root Locus (focusing on the critical poles within small window) when Increasing the Gains of the 2 TCSCs

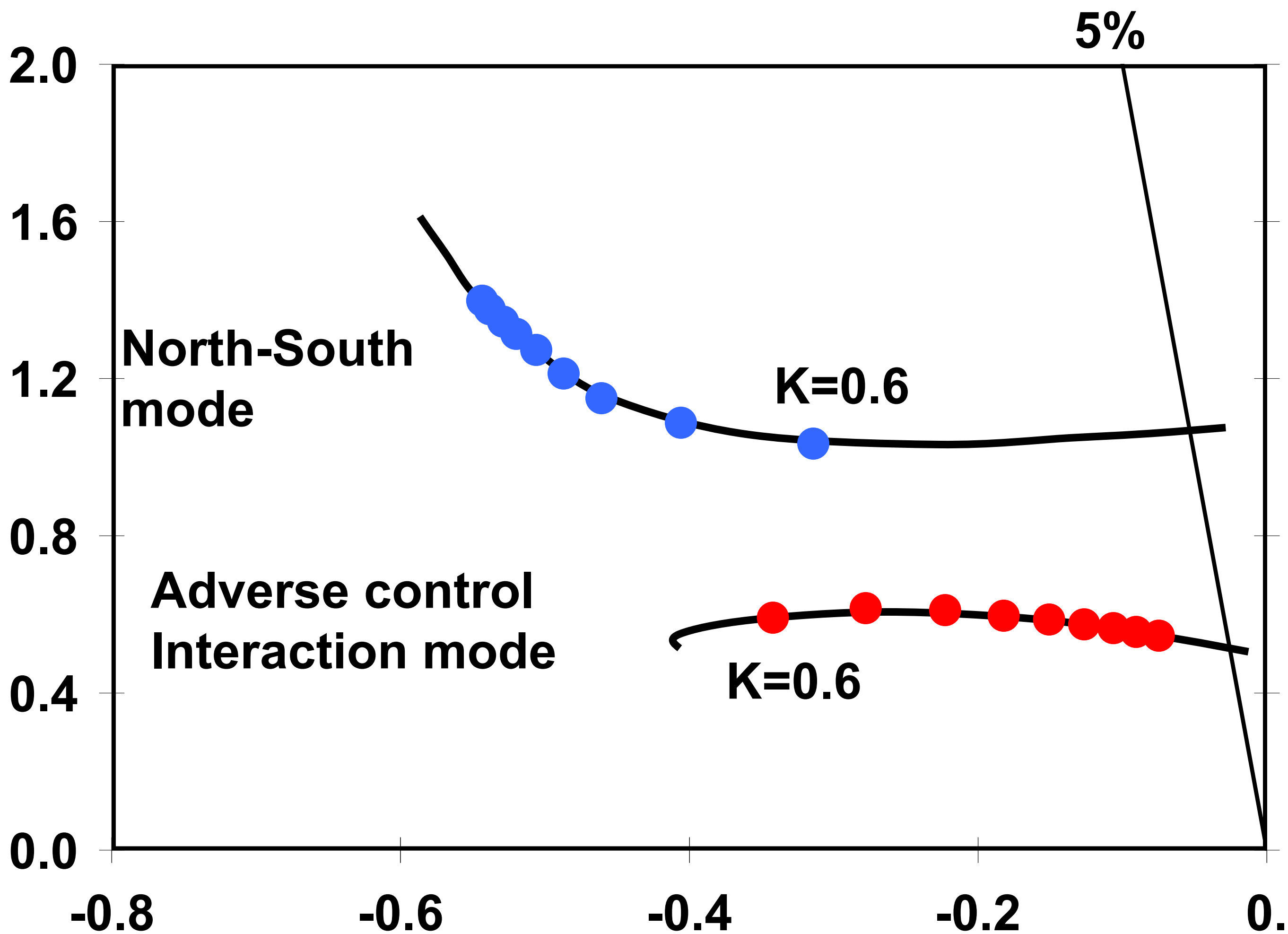

Root Locus (focusing on the critical poles within small window) when Increasing the Gains of the 2 TCSCs

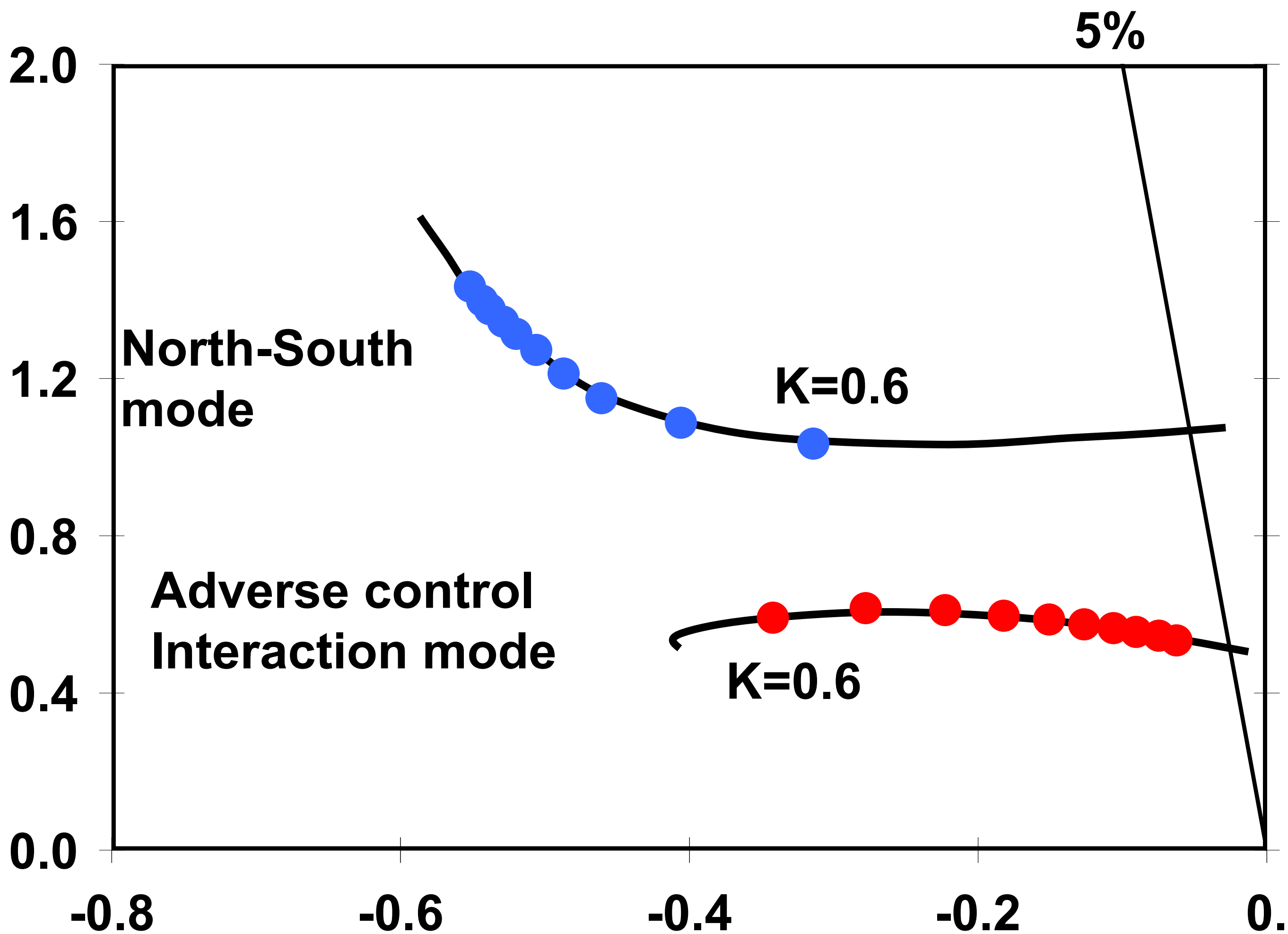

Root Locus (focusing on the critical poles within small window) when Increasing the Gains of the 2 TCSCs

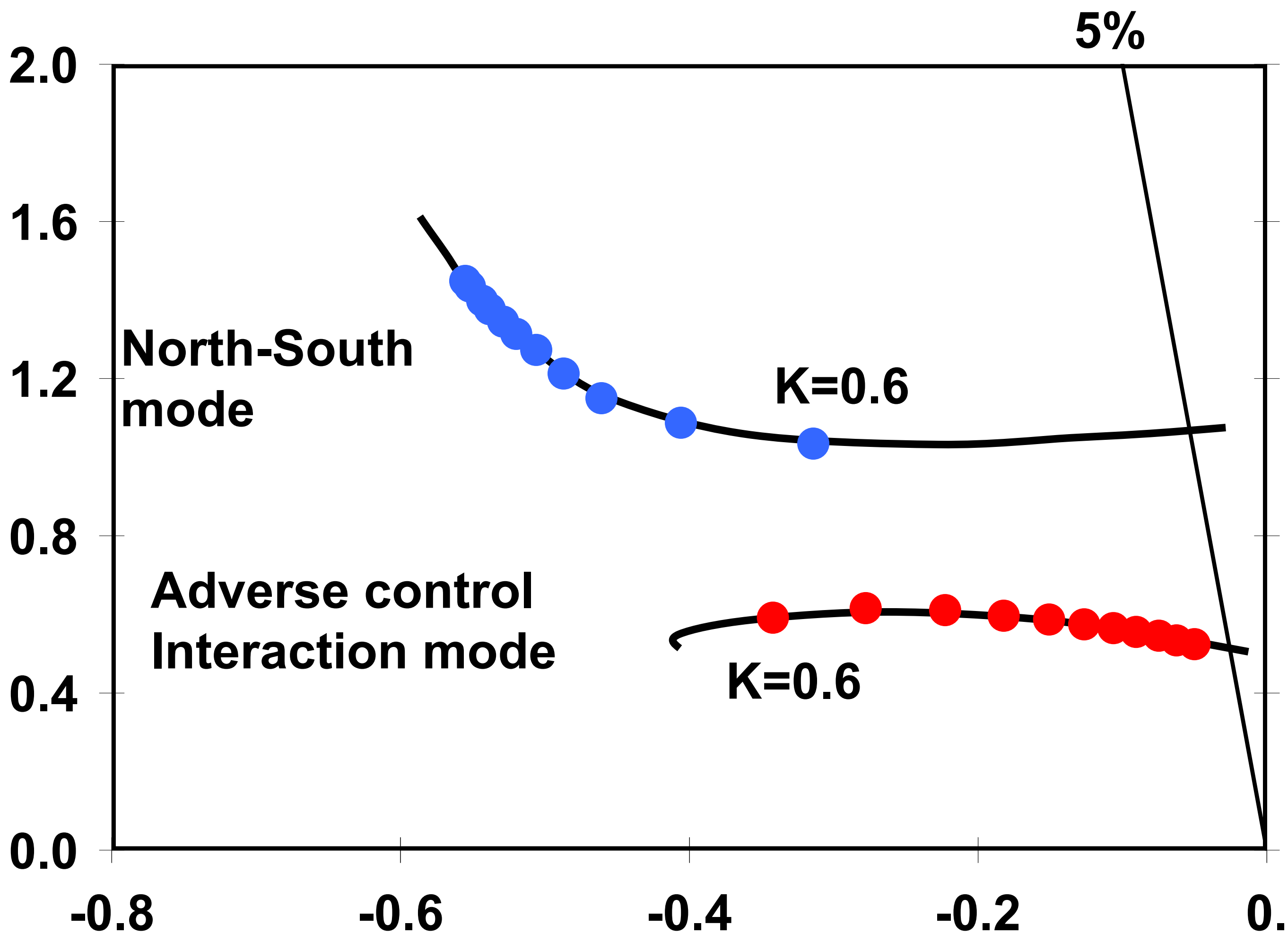

Root Locus (focusing on the critical poles within small window) when Increasing the Gains of the 2 TCSCs

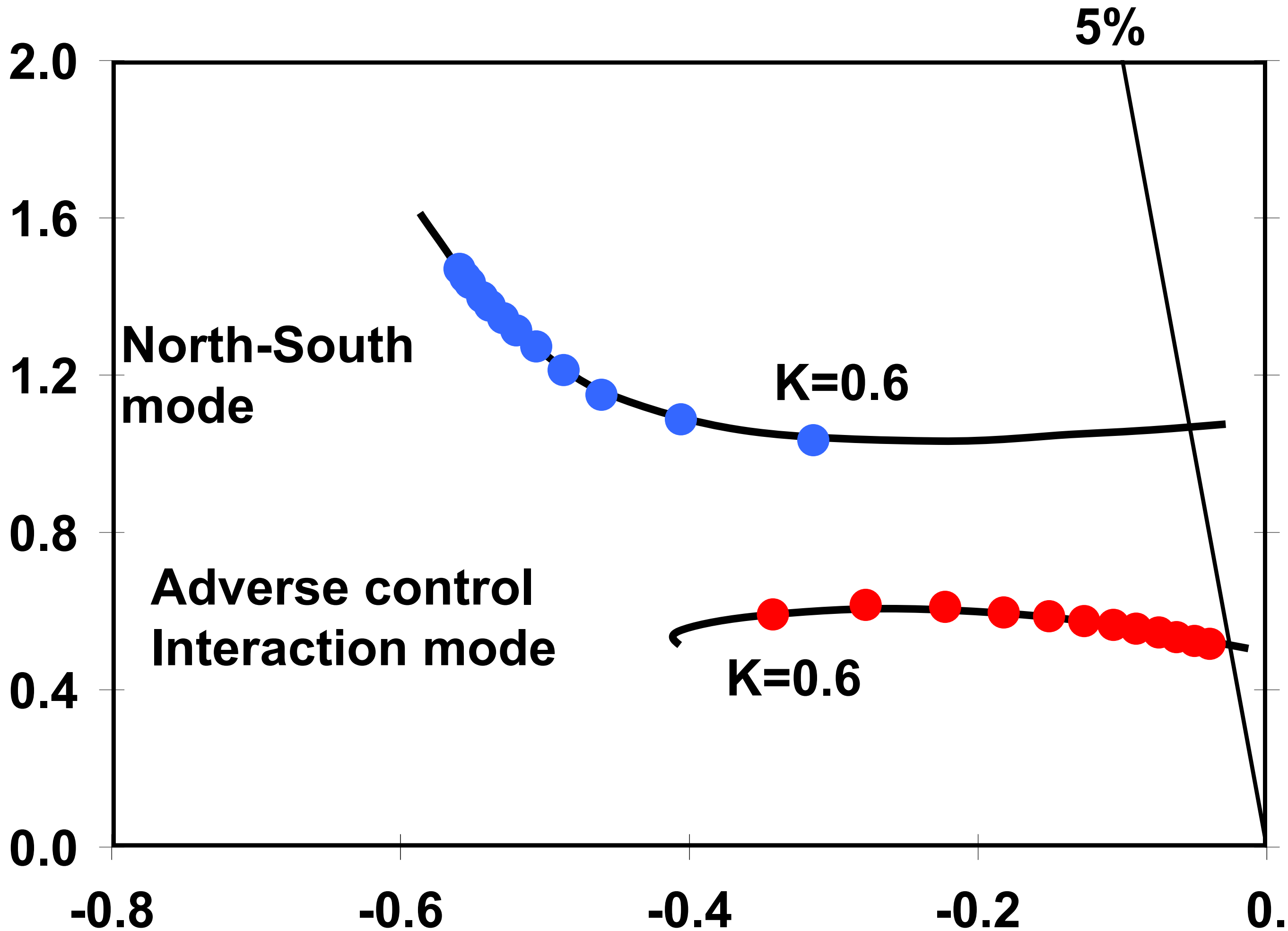

Root Locus (focusing on the critical poles within small window) when Increasing the Gains of the 2 TCSCs

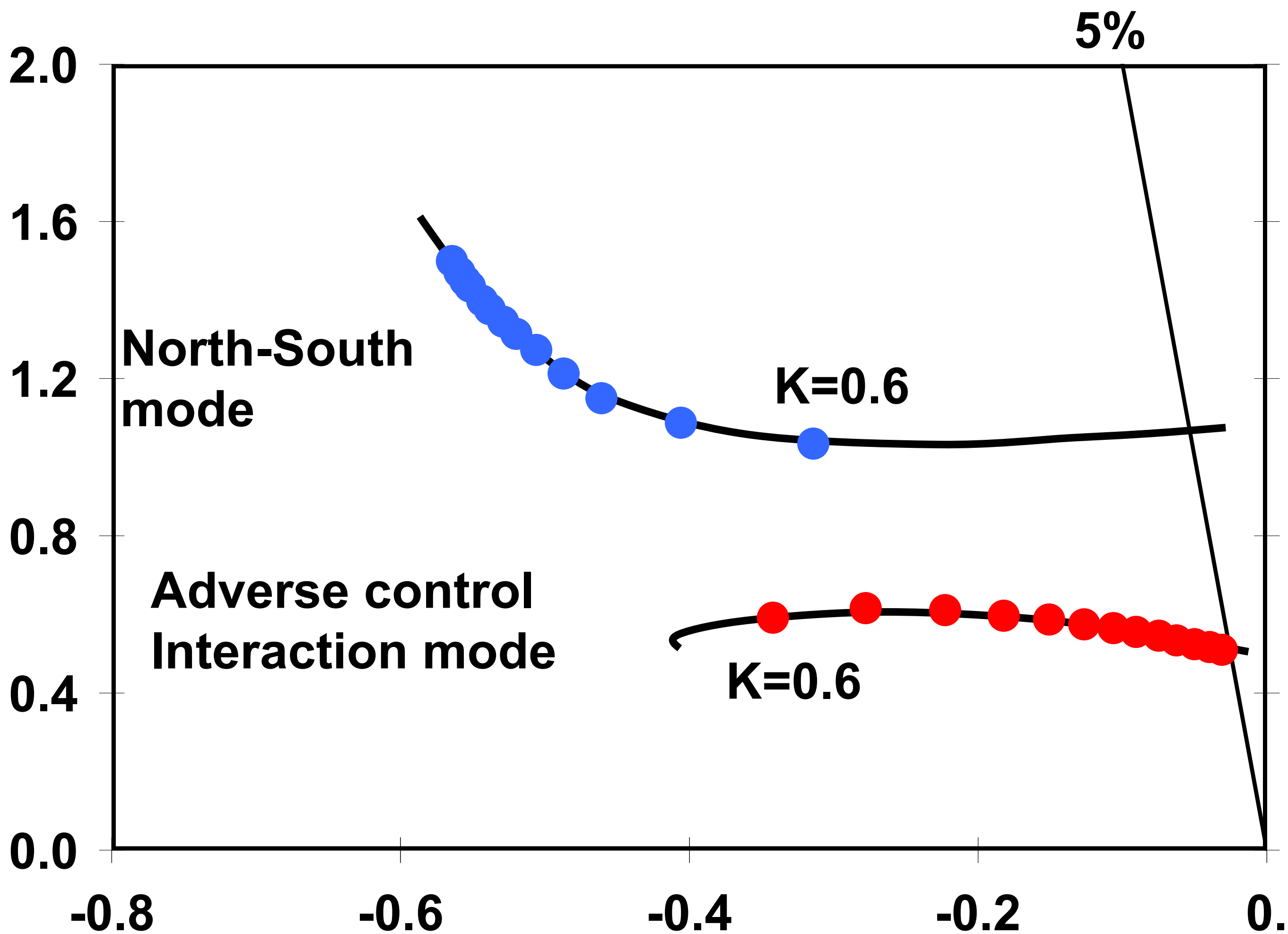

Root Locus (focusing on the critical poles within small window) when Increasing the Gains of the 2 TCSCs

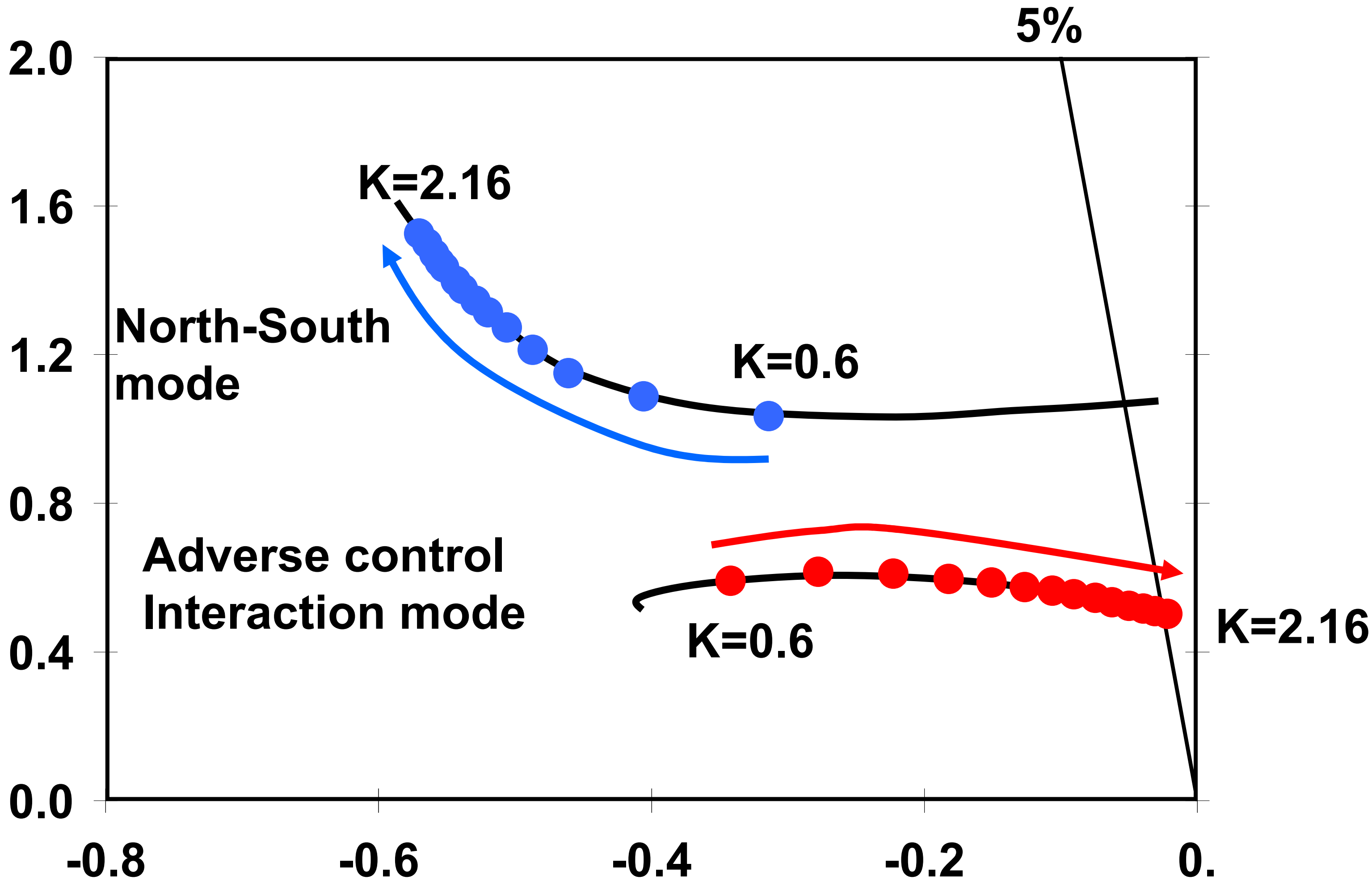

North-South System with no TCSCs

Interarea Mode: $\lambda = -0{,}0335 + j\,1{,}0787$ (f = 0,17 Hz, ζ = 3,11 %)

Mode Shape for Generator Rotor Speeds

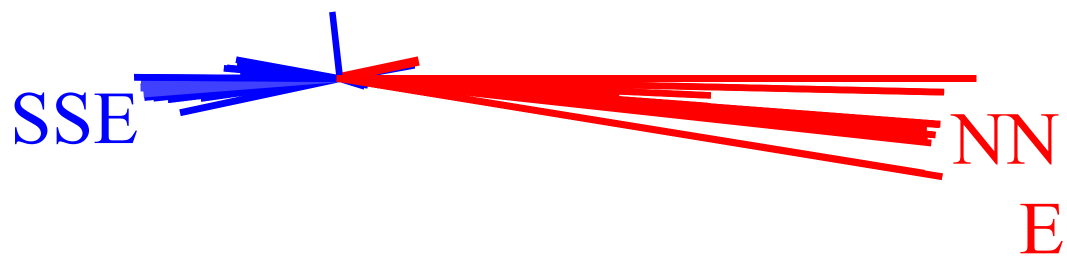

Step Response (N-S Tie line Power)

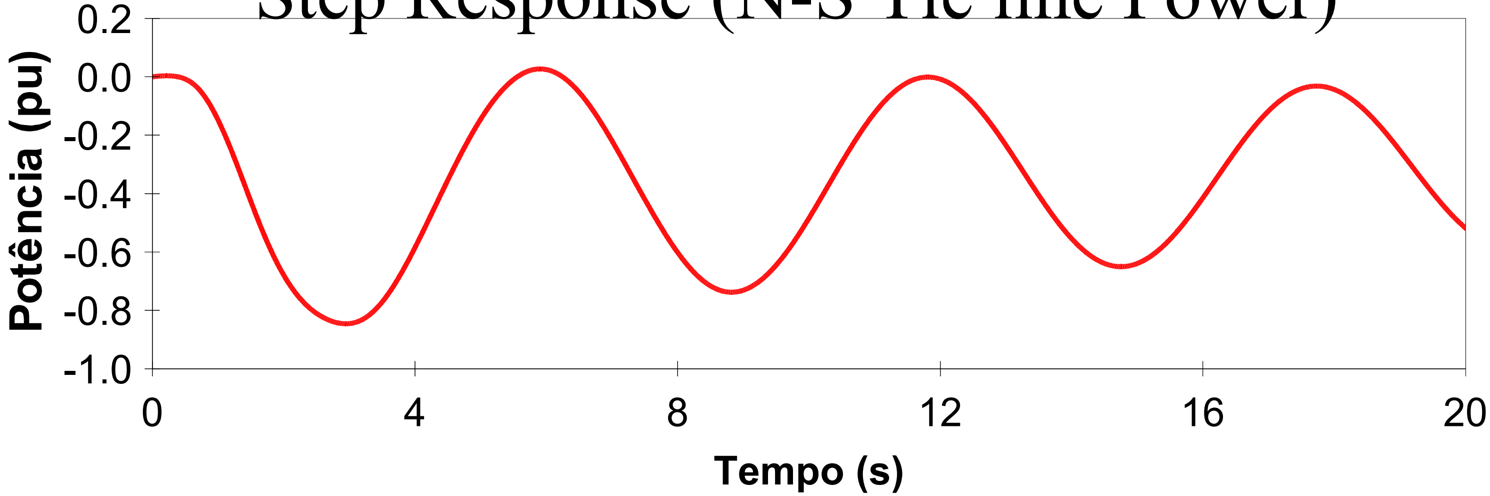

North-South System with 2 TCSCs

Inter-area mode without TCSCs: $\lambda = -0{,}0335 + j\,1{,}0787$ ($\zeta = 3{,}11\%$)

Inter-area mode with TCSCs: $\lambda = -0{,}318 + j\,1{,}044$ ($\zeta = 29{,}14\ \%$)

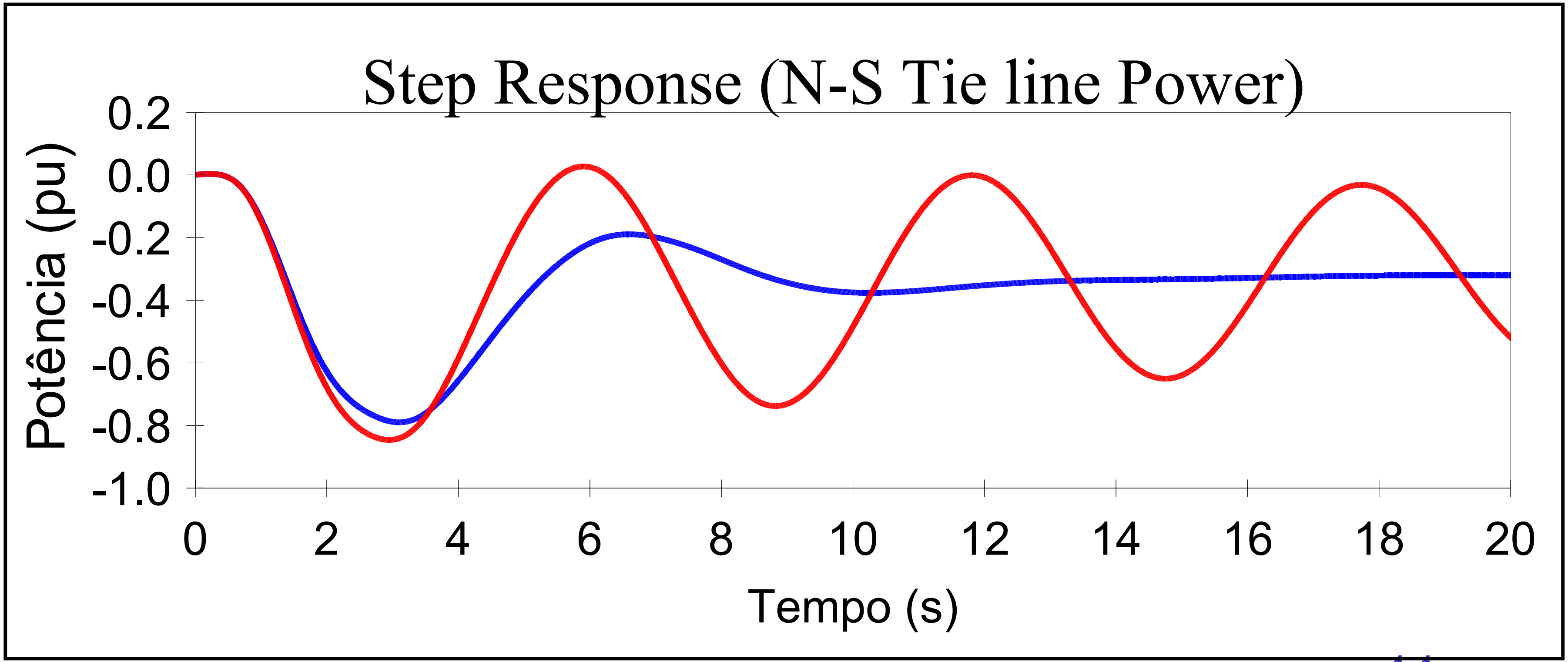

Computation of S. Signal Stability Boundaries

- Different algorithms, heuristics, parameter limits and boundaries
  - Change of a single parameter (Newton)
  - Change of multiple parameters (Lagrange)
  - Step-length control
  - Maximum and minimum limits for parameter values
  - Small-signal security boundaries

- Cases investigated by the authors
  - Simultaneous change in the gains of the 2 TCSCs
  - Independent changes in the gains of the 2 TCSCs
  - Varying other system parameters

Hopf Bifurcation Results

Determining K_{min} for 5% Security Boundary

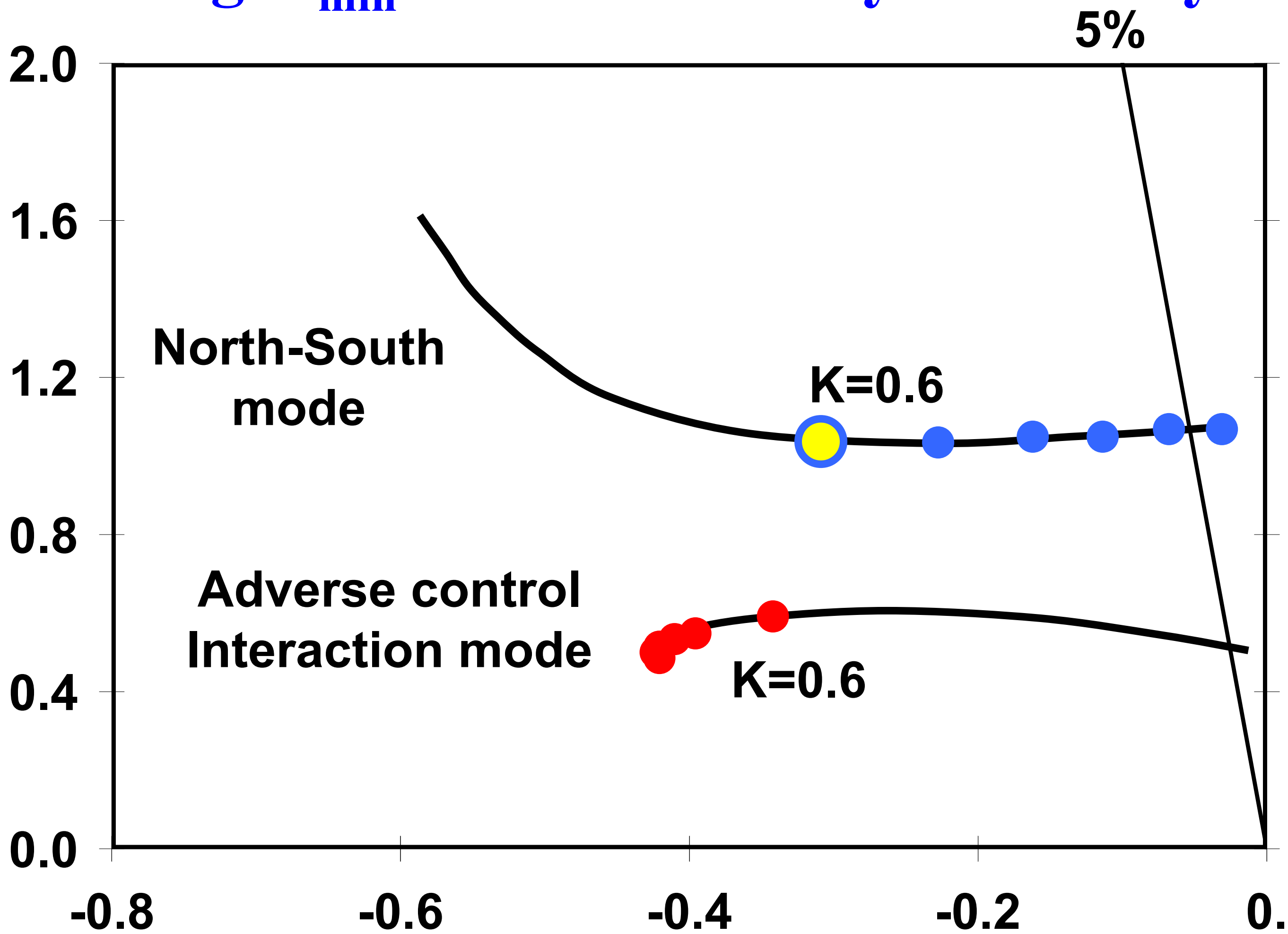

Hopf Bifurcation Results

Determining K_{min} for 5% Security Boundary

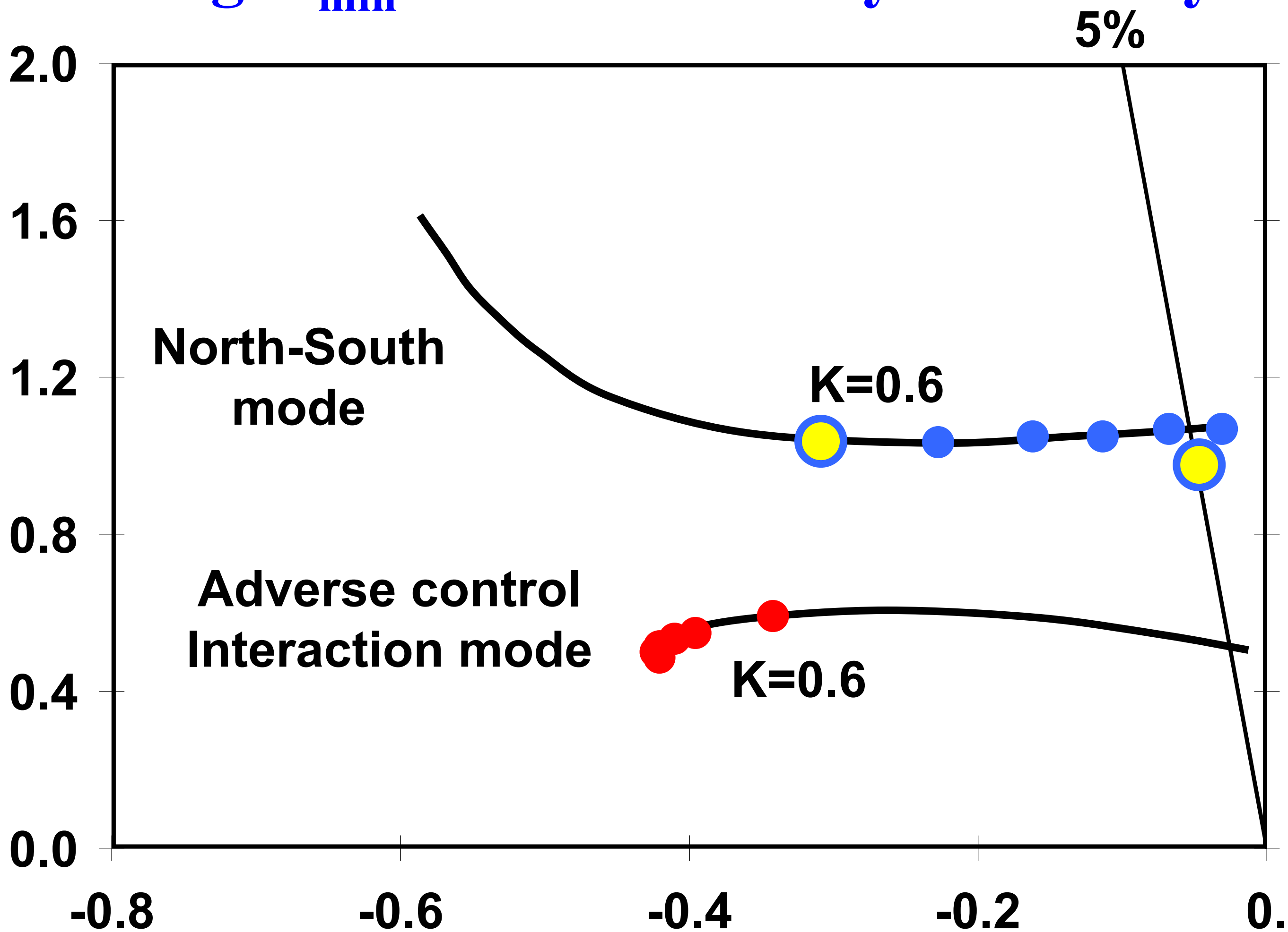

Hopf Bifurcation Results

Determining K_{min} for 5% Security Boundary

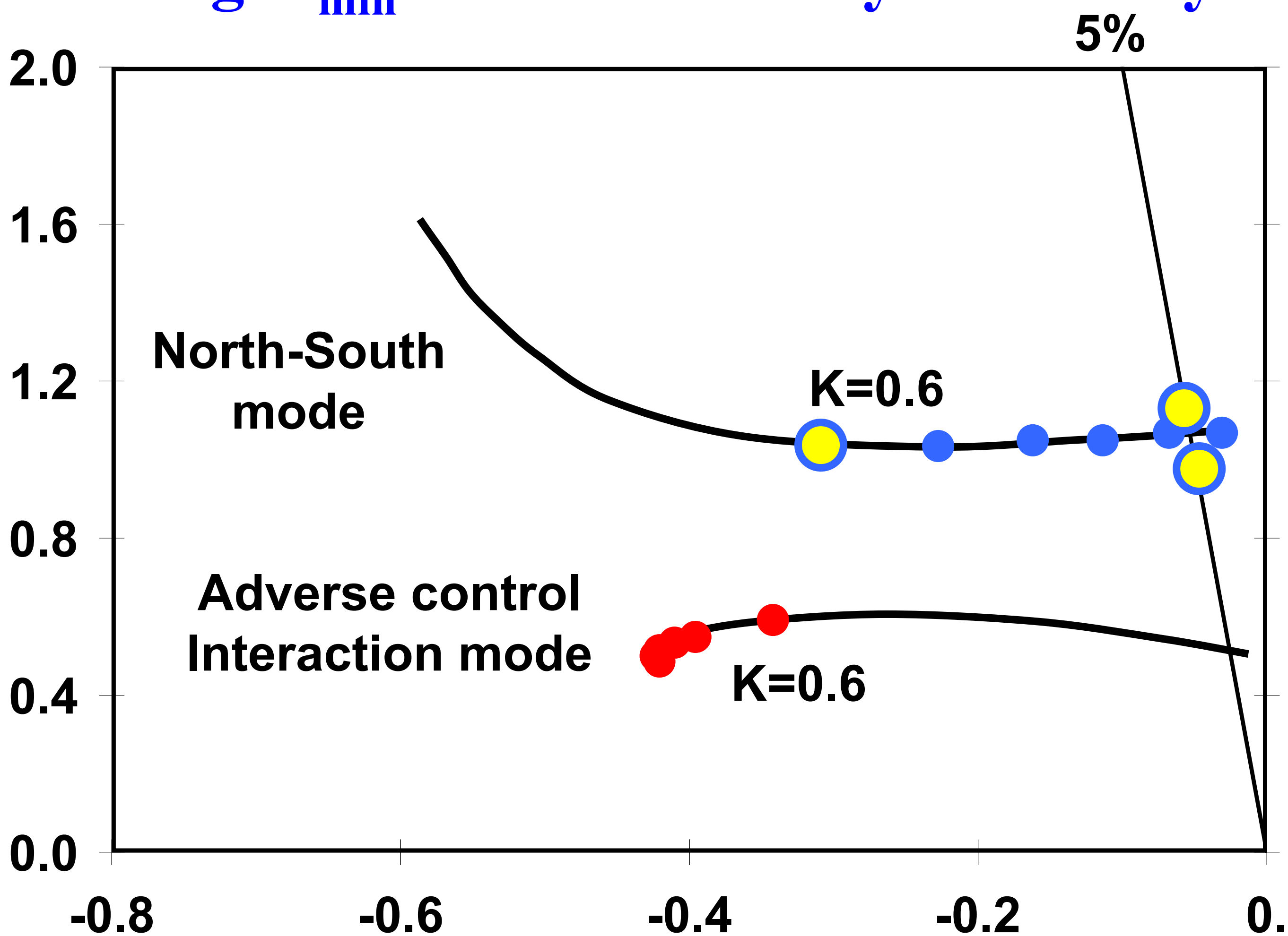

Hopf Bifurcation Results

Determining K_{min} for 5% Security Boundary

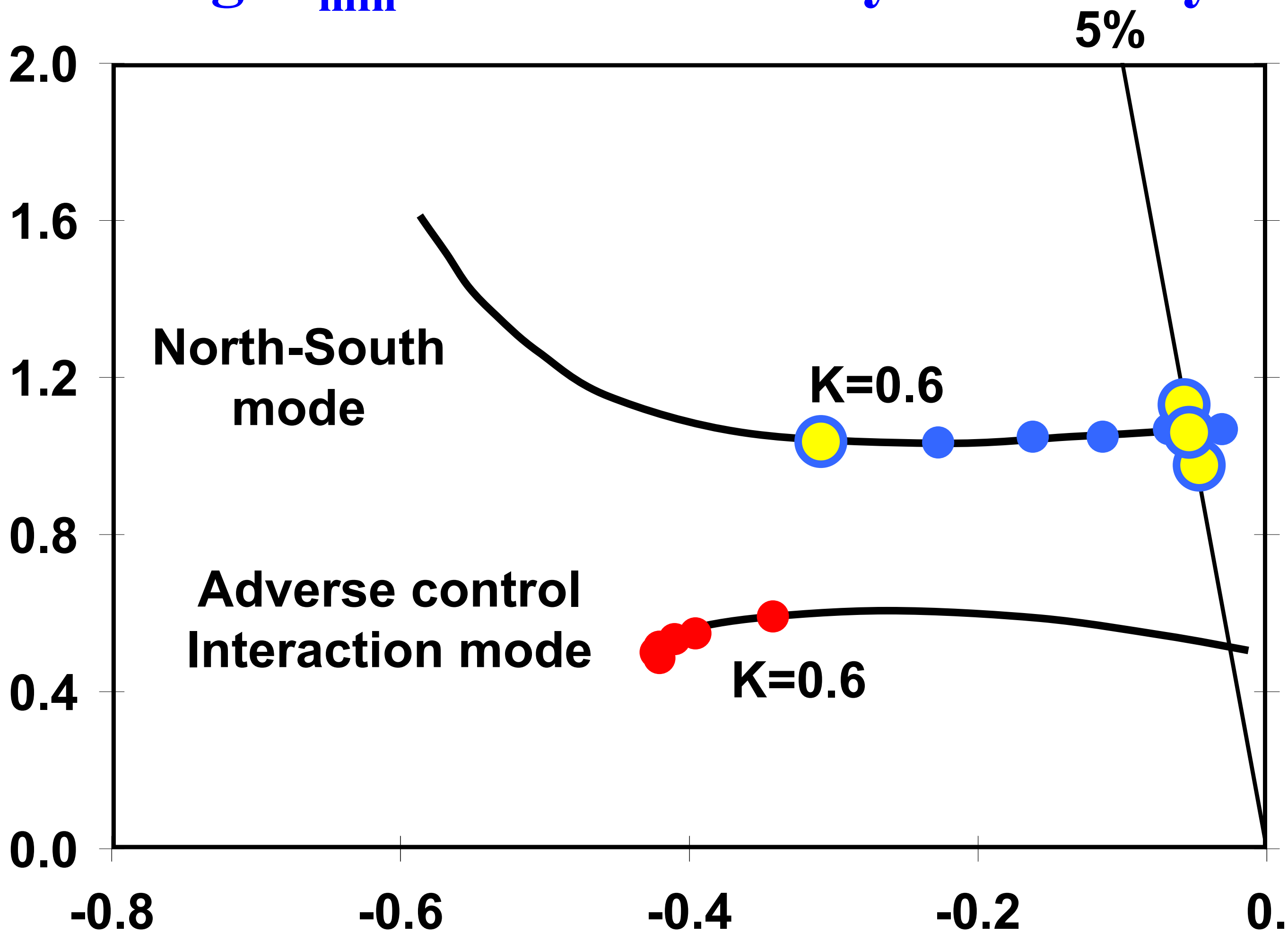

Hopf Bifurcation Results

Determining K_{min} for 5% Security Boundary

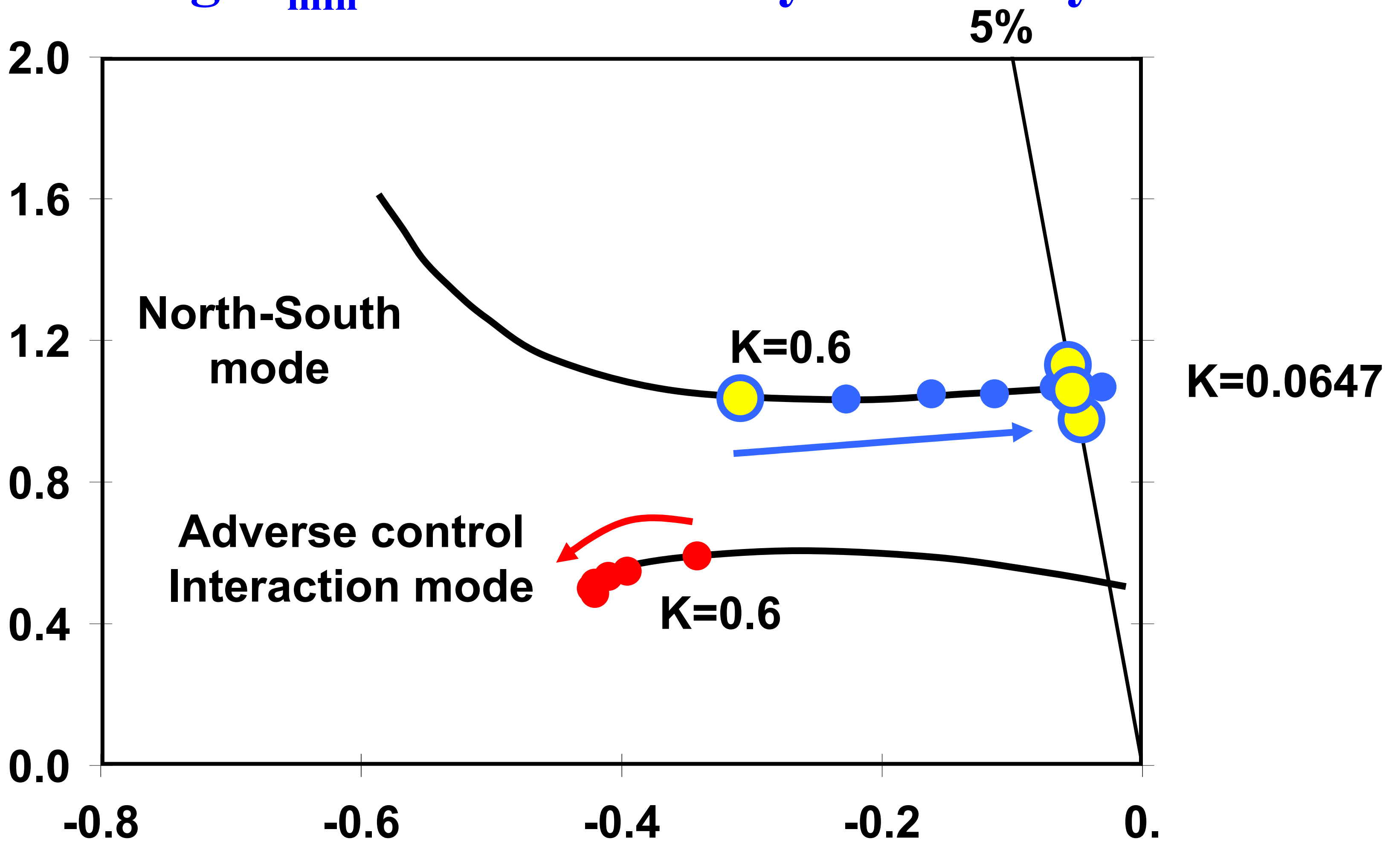

Hopf Bifurcation Results

Determining K_{max} for 5% Security Boundary

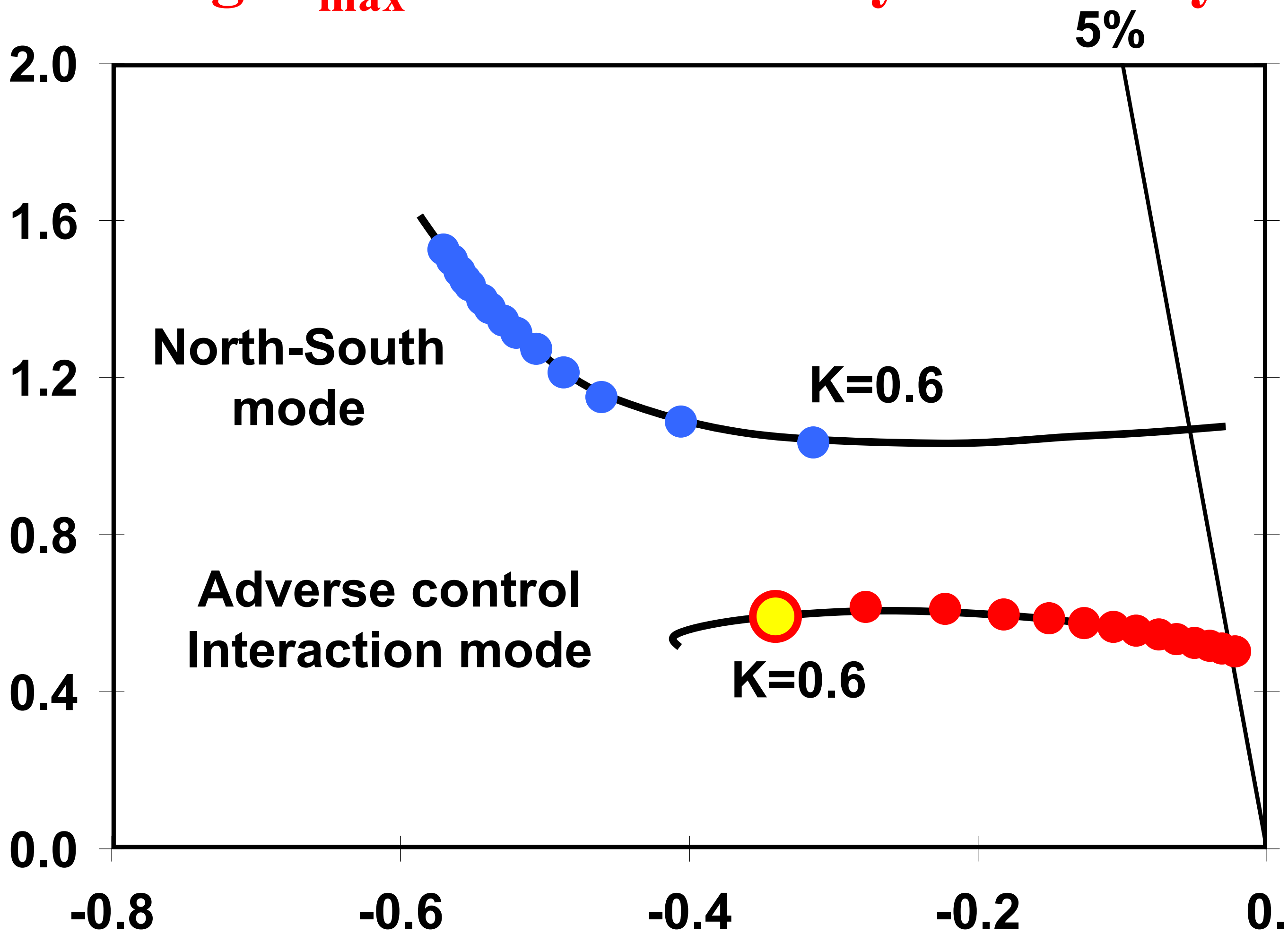

Hopf Bifurcation Results

Determining K_{max} for 5% Security Boundary

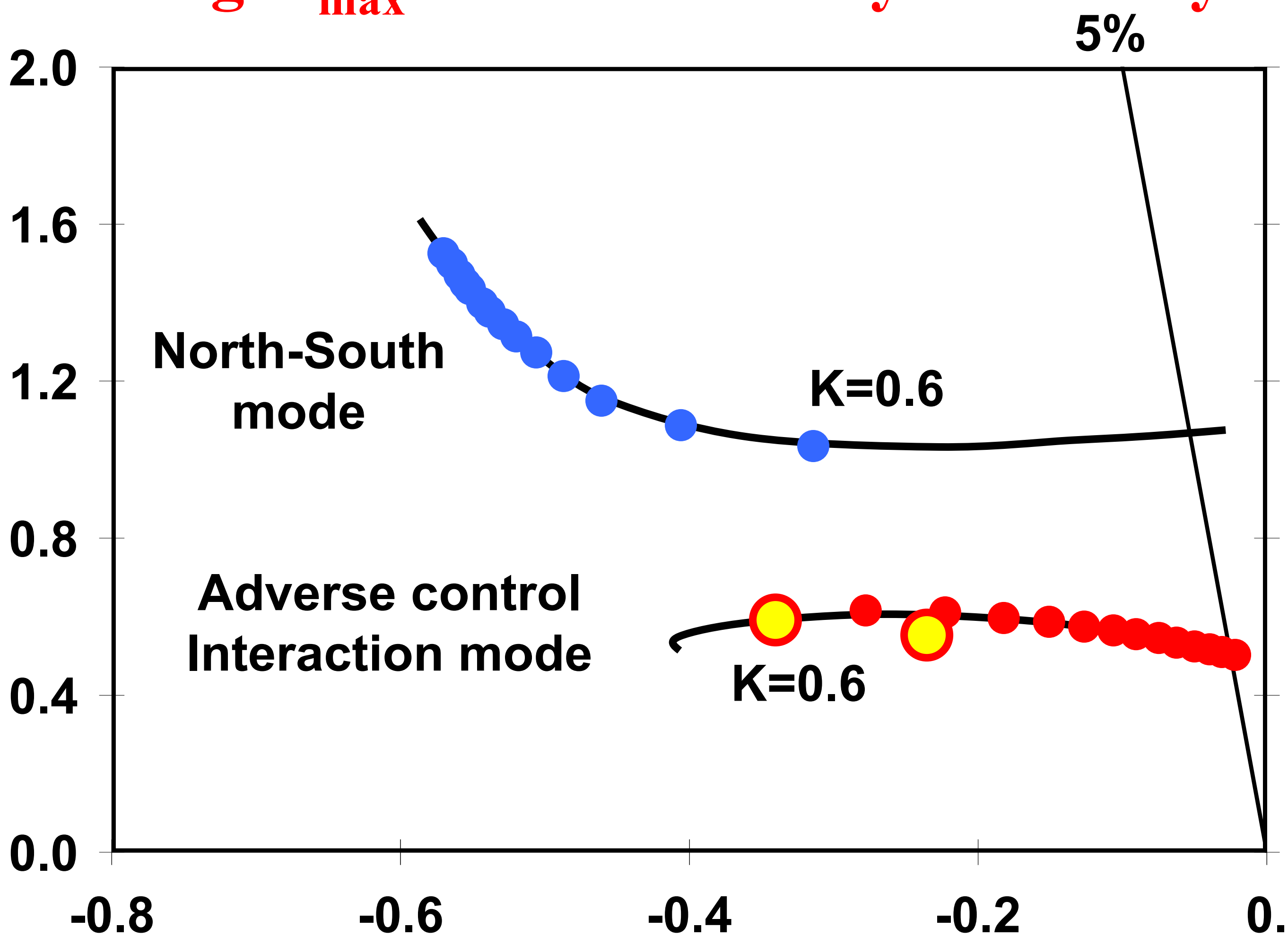

Hopf Bifurcation Results

Determining K_{max} for 5% Security Boundary

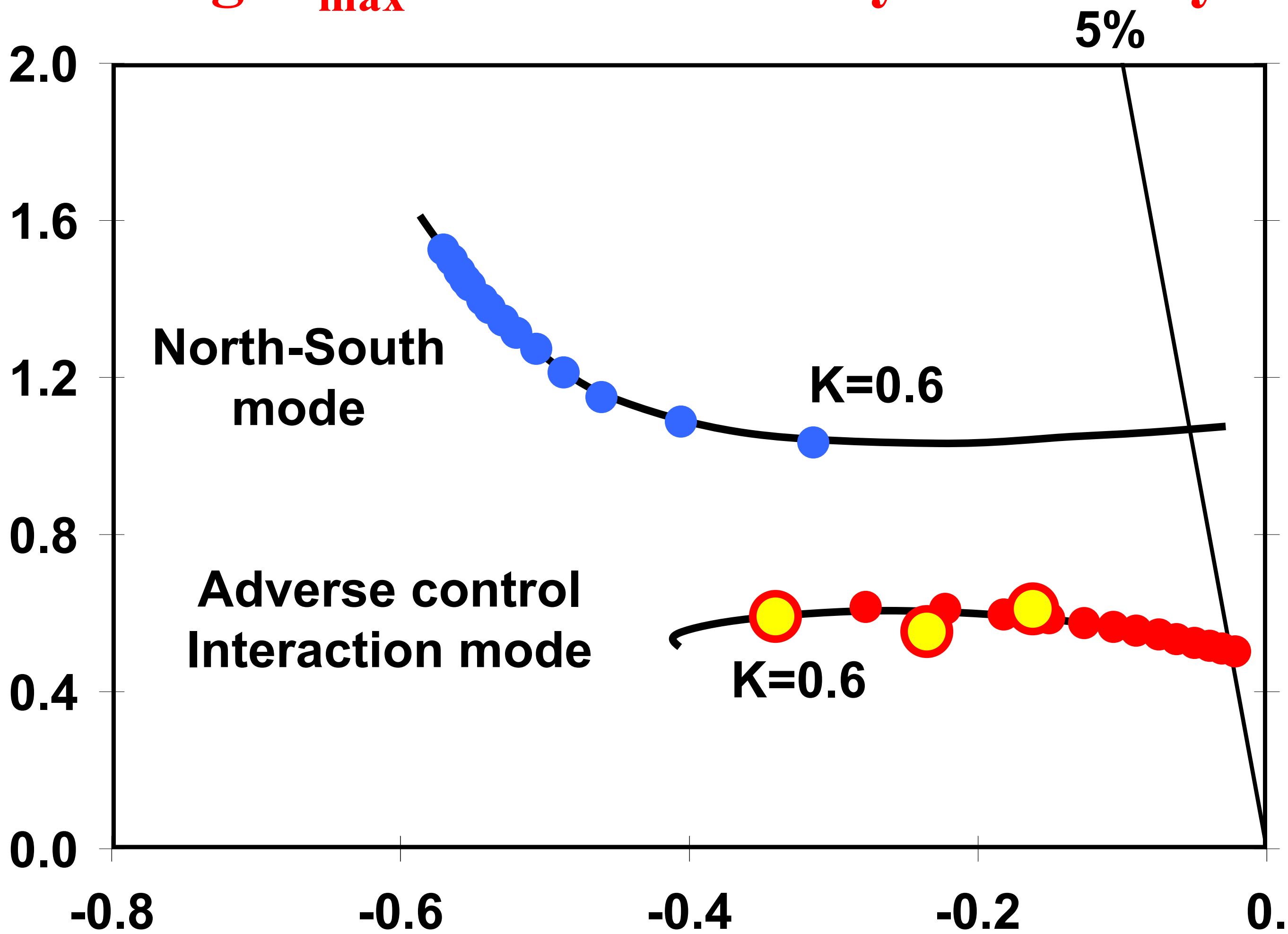

Hopf Bifurcation Results

Determining K_{max} for 5% Security Boundary

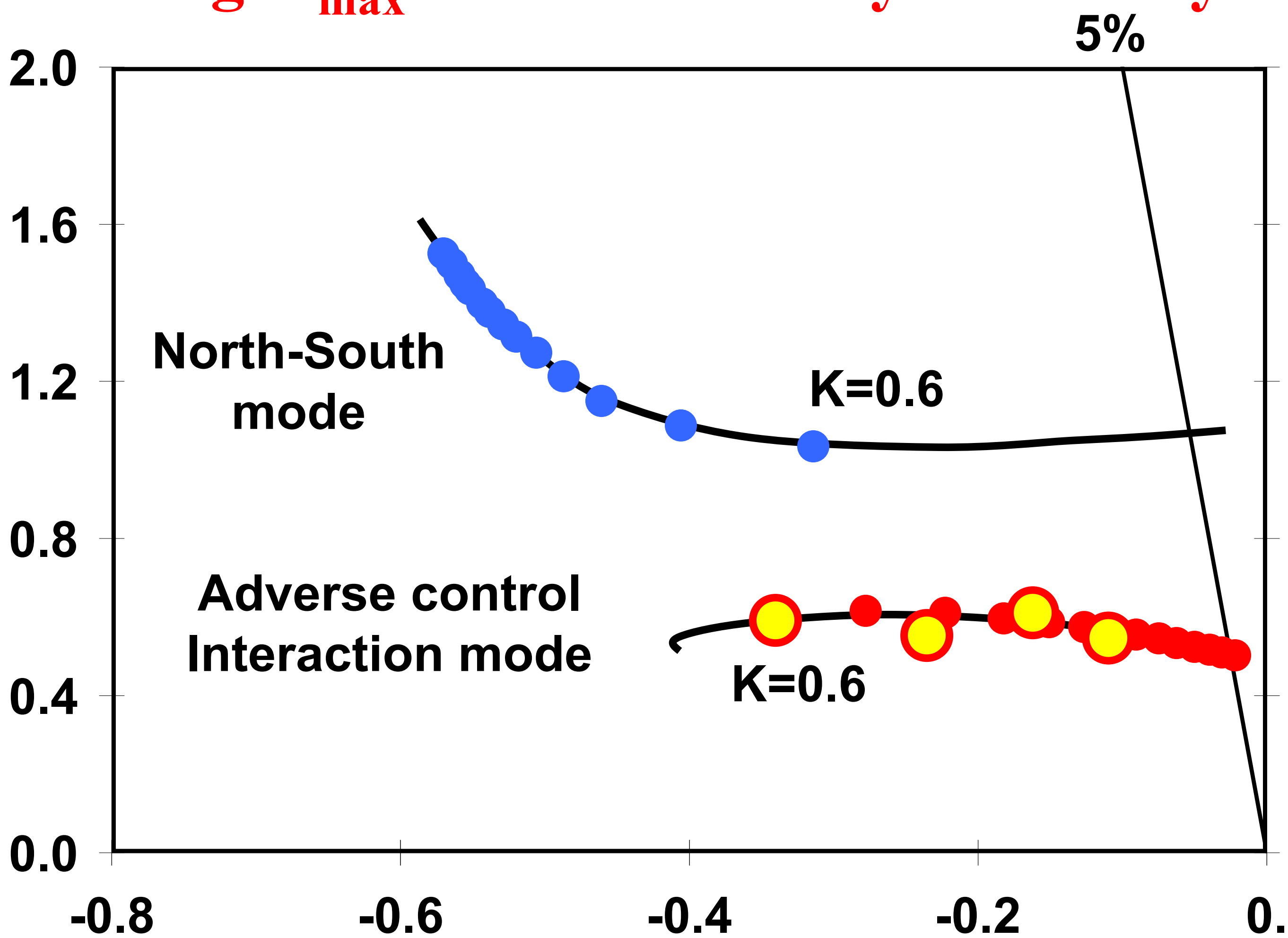

Hopf Bifurcation Results

Determining K_{max} for 5% Security Boundary

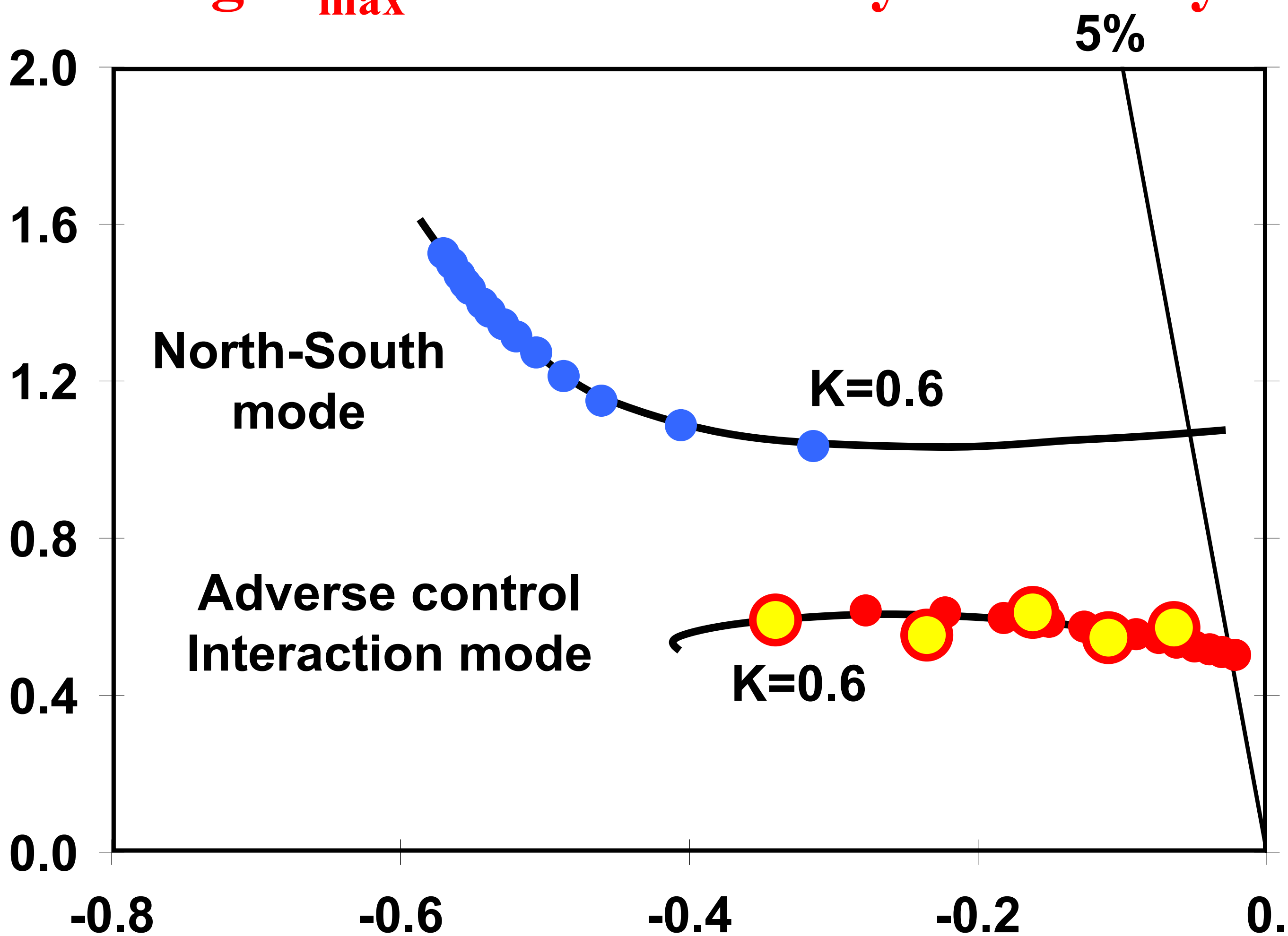

Hopf Bifurcation Results

Determining K_{max} for 5% Security Boundary

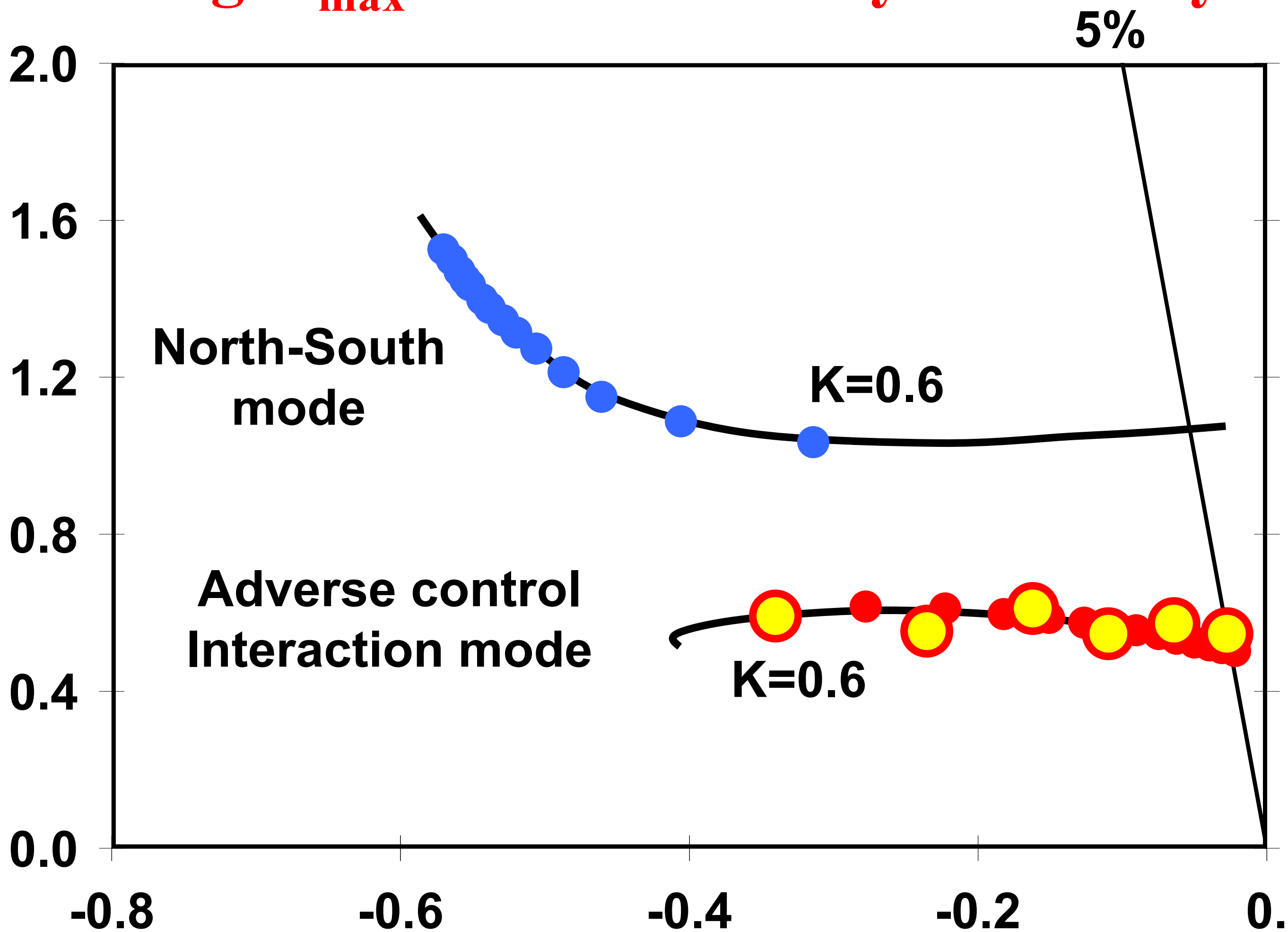

Hopf Bifurcation Results

Determining K_{max} for 5% Security Boundary

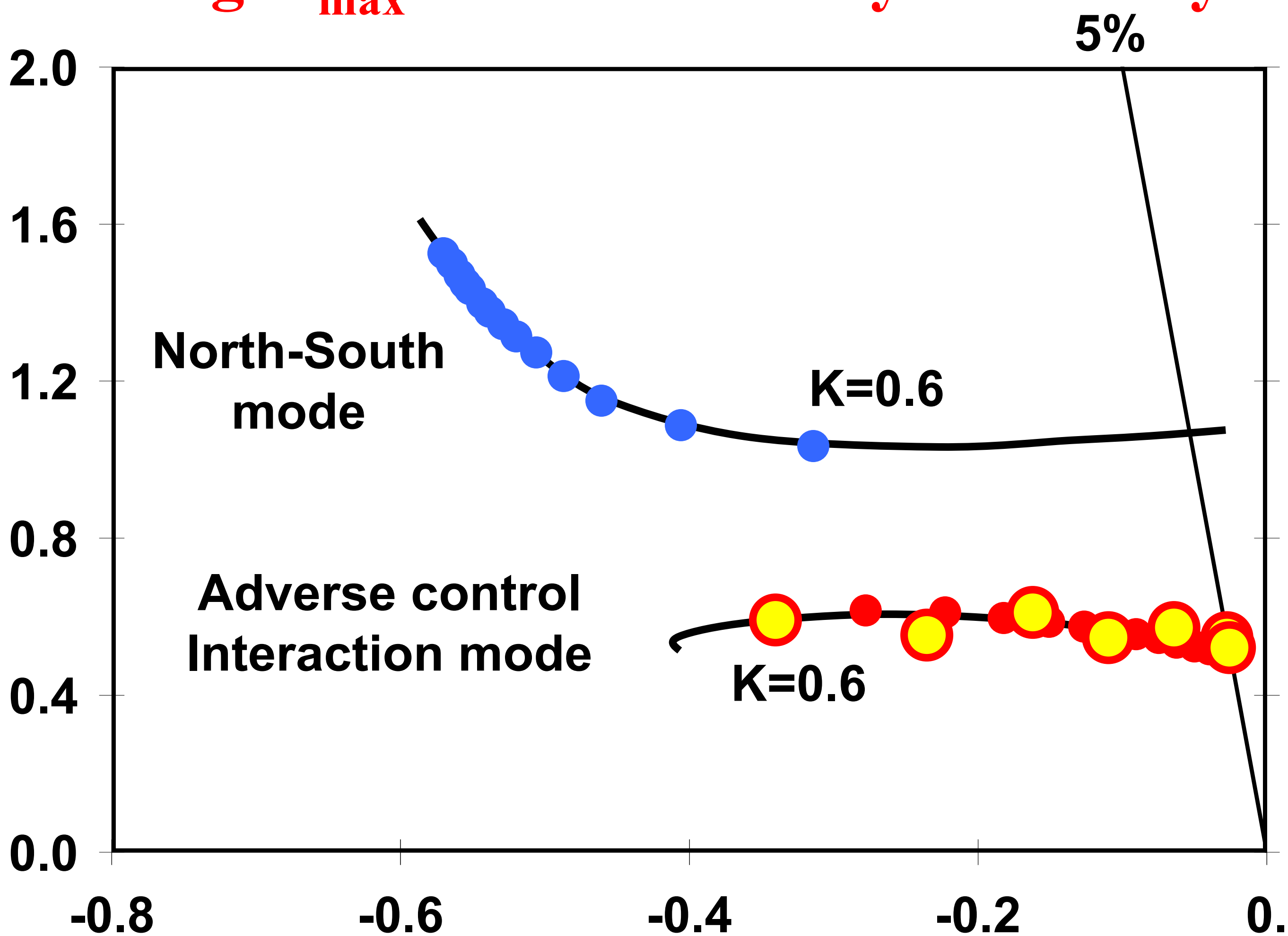

Hopf Bifurcation Results

Determining K_{max} for 5% Security Boundary

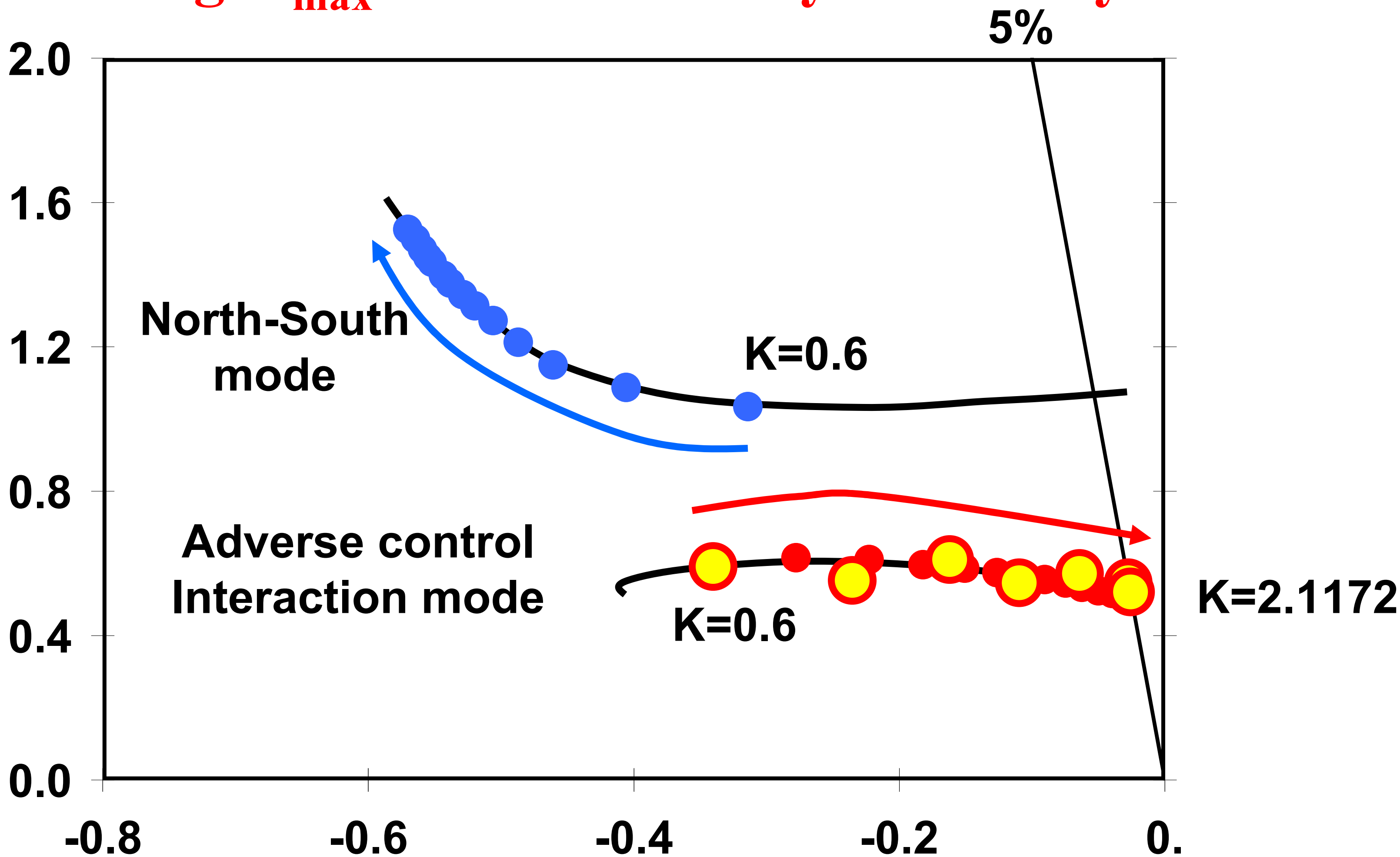

Hopf Bifurcations Results

- Two crossings of the security boundary were found, for POD gains far away from the nominal values (**K_{nom} = 0.6 pu**):

$$\mathbf{2.1172 > K > 0.0647}$$

- Computational cost of Hopf bifurcation algorithm
  - Single-parameter changes : 0.16 s (per iteration)
  - Multiple-parameter changes : 0.35 s (per iteration)

Step Responses for Different TCSC Gains: $K_{nom} = 0.6$ and $K_{min} = 0.06471$

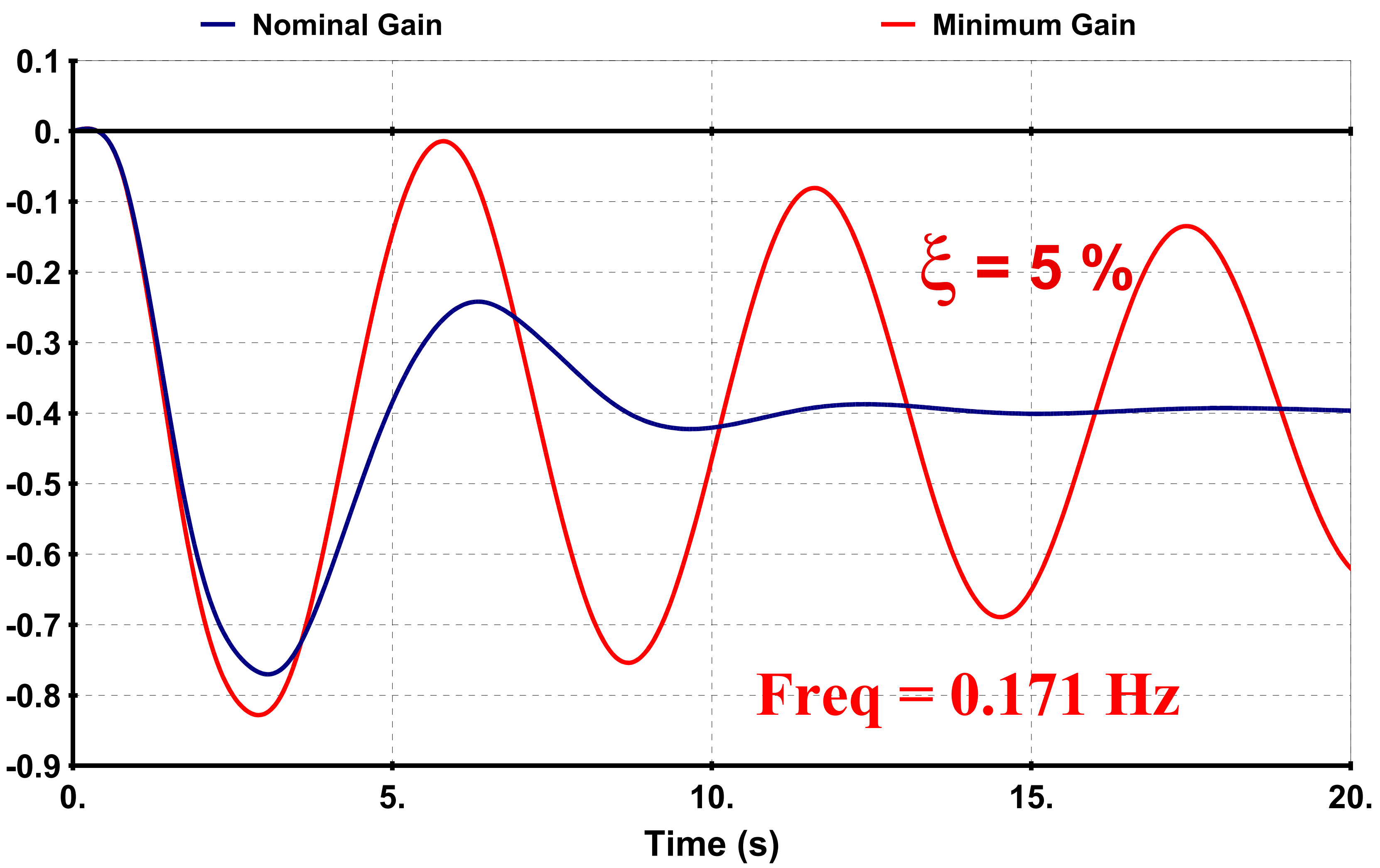

Step Responses for Different TCSC Gains: $K_{nom} = 0.6$ and $K_{max} = 2.1172$

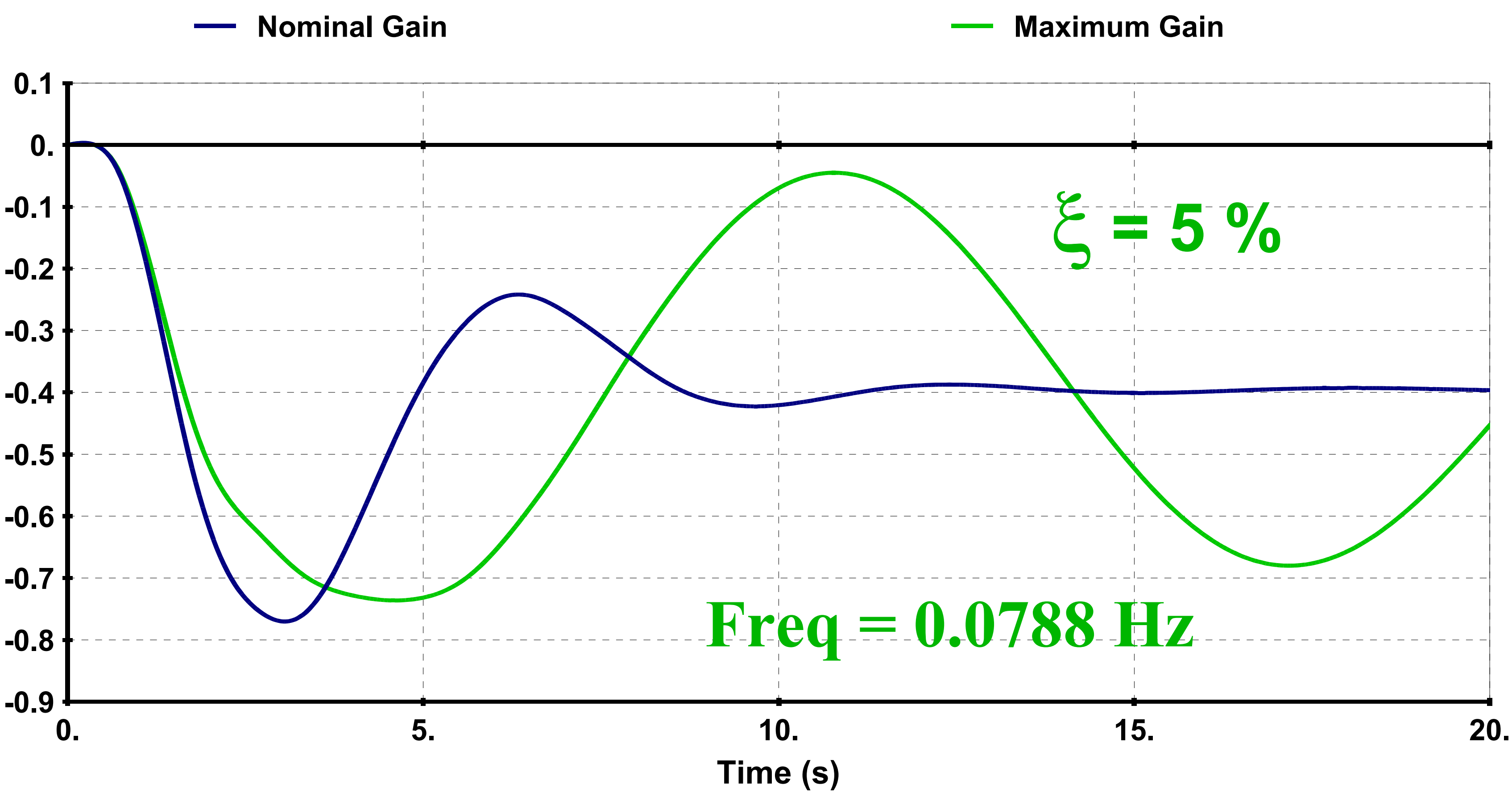

Jacobian Matrix for Brazilian System Model (13, 062 equations with 48,626 non-zeros)

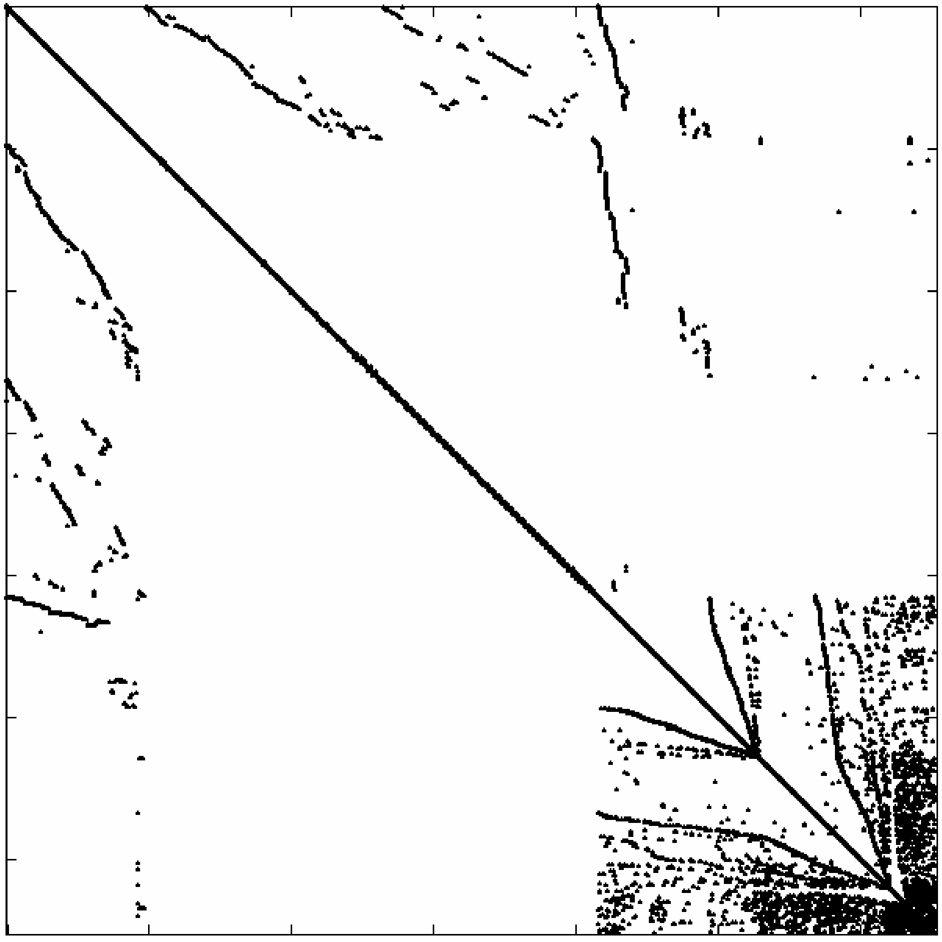

Eigenvalue (Pole) Spectrum for Brazilian North-South System (1,676 eigenvalues)

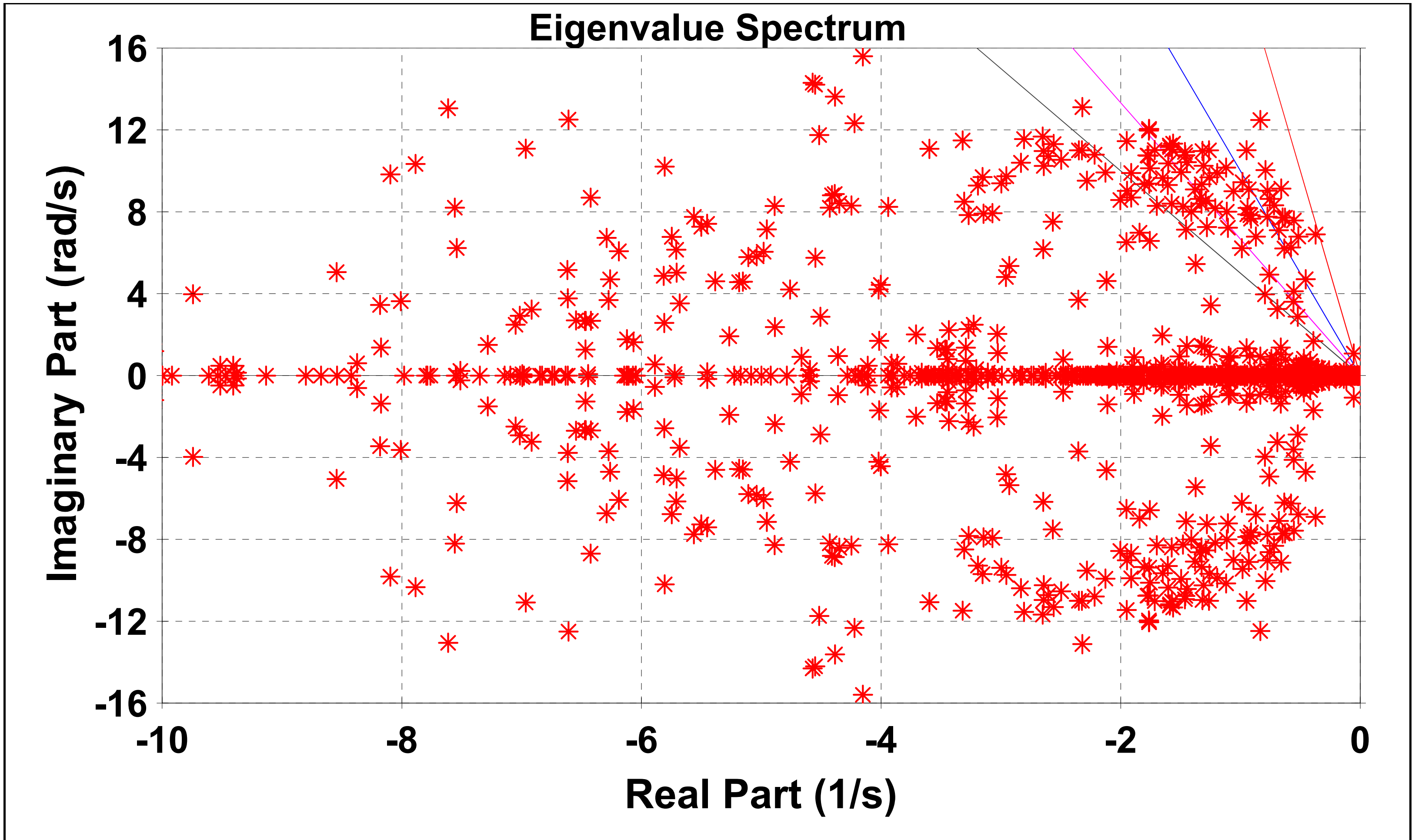

Hopf Matrix and its LU Factors (26,127 lines)

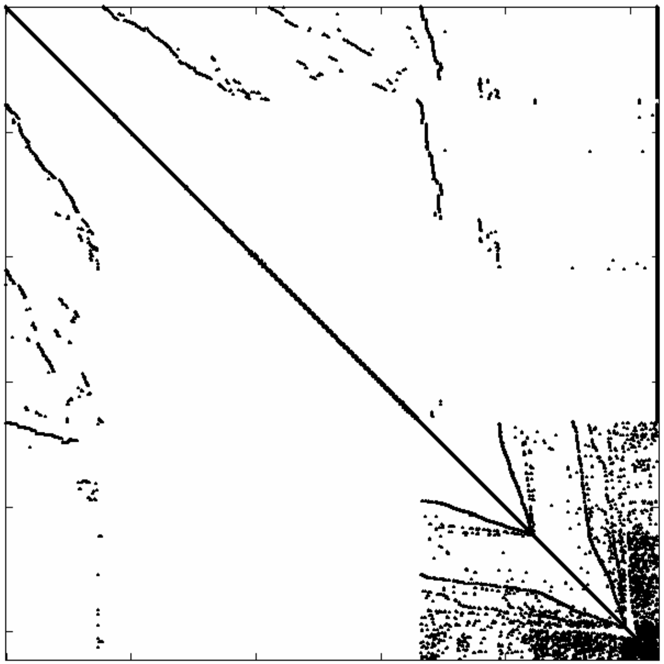

108,288 non-zeros

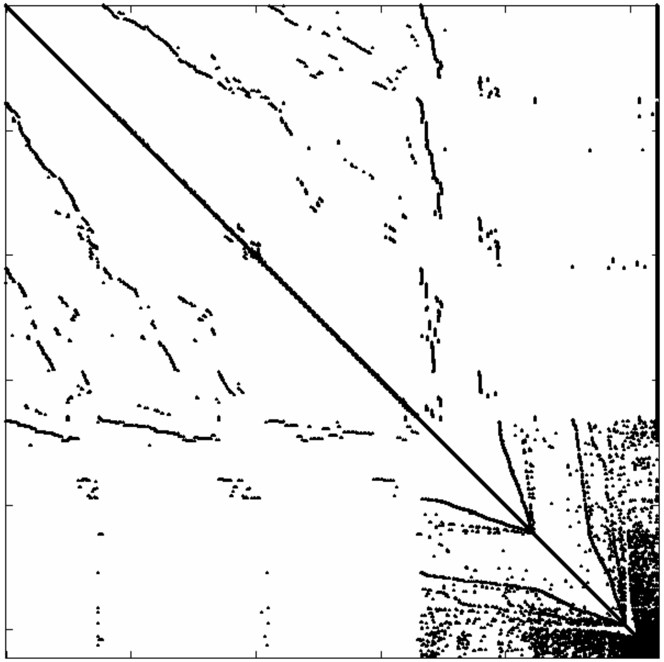

256,915 non-zeros

Convergence Performance of the Hopf Algorithm (K_{min} Solution)

Iteration	Eigenvalue Estimate	Gains of the two PODs
0	$-0.31793 + j\,1.0437$	0.600000
1	$-0.049219 + j\,0.98315$	0.264483
2	$-0.055743 + j\,1.1135$	0.00911156
3	$-0.053862 + j\,1.0759$	0.0596167
4	$-0.053750 + j\,1.0736$	0.0646849
5	$-0.053749 + j\,1.0736$	0.0647119
6	$-0.053749 + j\,1.0736$	0.0647119

Convergence Performance of the Hopf Algorithm (K_{max} Solution)

Iteration	Eigenvalue Estimate	POD Gains	ζ (%)
0	$-0.34641 + j\,0.57961$	0.600000	51.30
1	$-0.28045 + j\,0.61841$	0.727598	41.30
2	$-0.19803 + j\,0.60087$	0.864511	31.30
3	$-0.12364 + j\,0.56710$	1.14716	21.30
4	$-0.059773 + j\,0.52549$	1.59247	11.30
5	$-0.024886 + j\,0.49710$	2.04841	5
6	$-0.024790 + j\,0.49518$	2.11759	5
7	$-0.024789 + j\,0.49516$	2.11725	5

Pole Spectrum of 1,676-State System

Small window near the origin is shown enlarged in next 3 slides

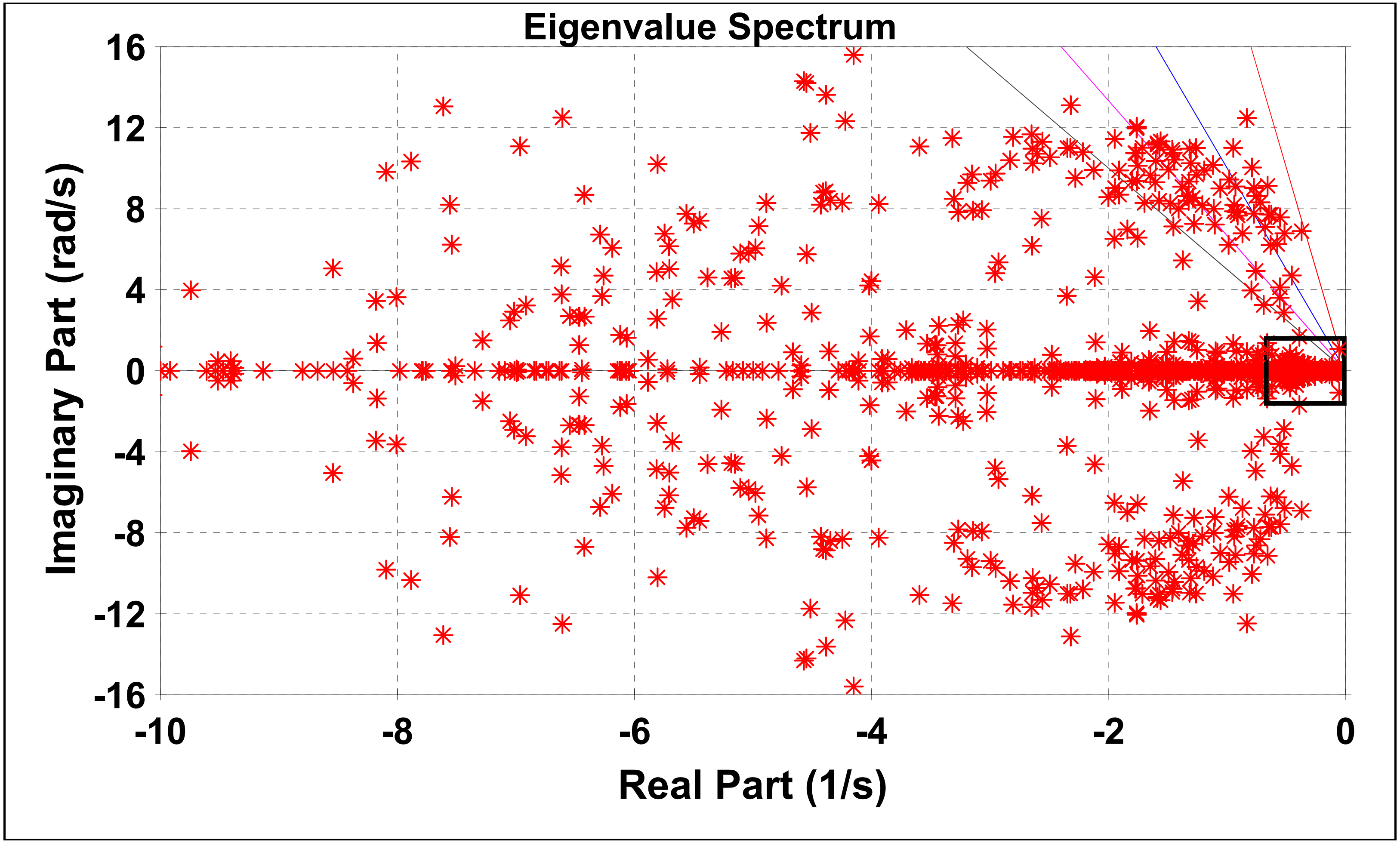

Enlarged View of Small Window in the 1676-Pole Spectrum, for $K_{nom} = 0.6$

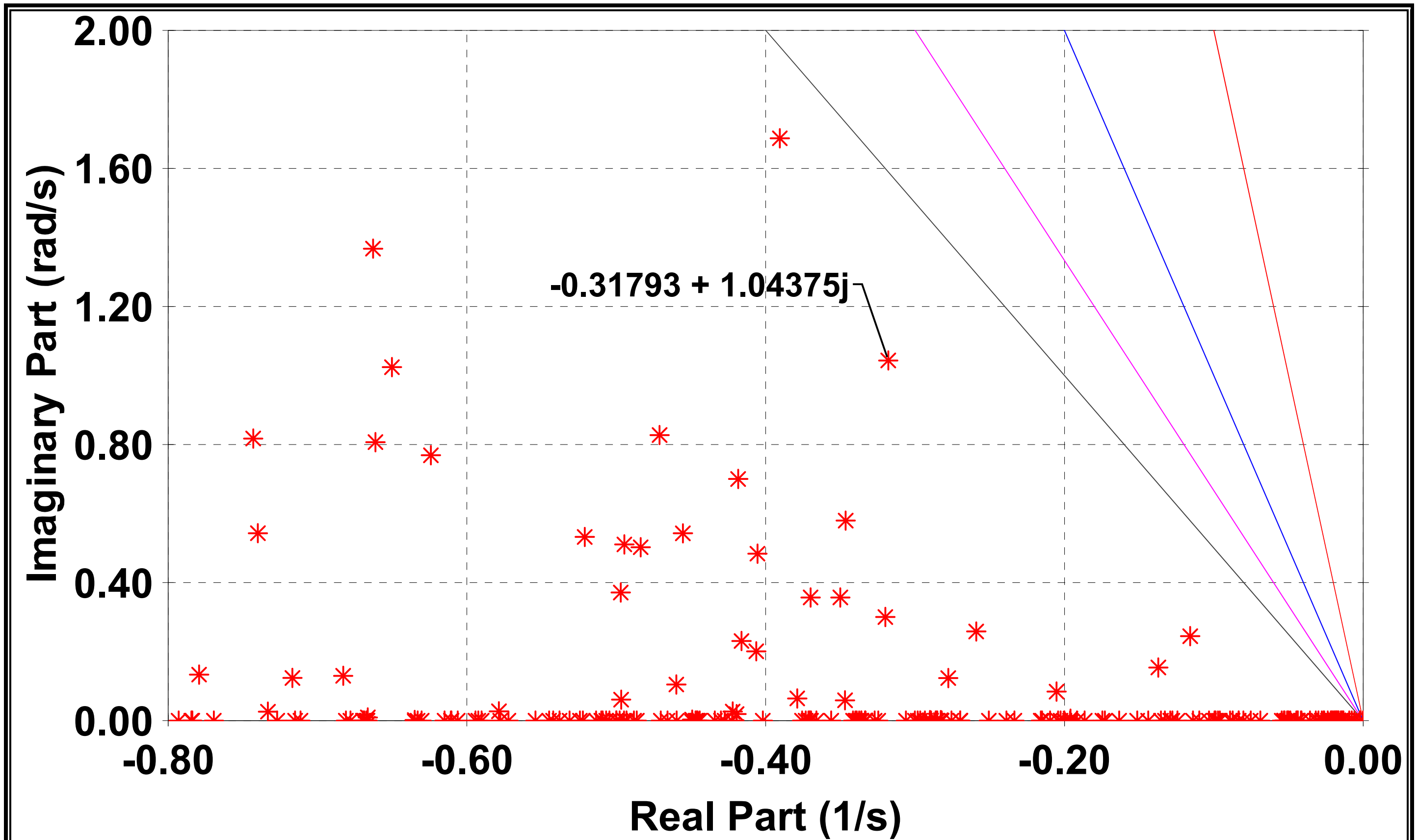

Enlarged View of Small Window in the 1676-Pole Spectrum, for $K_{min} = 0.06471$

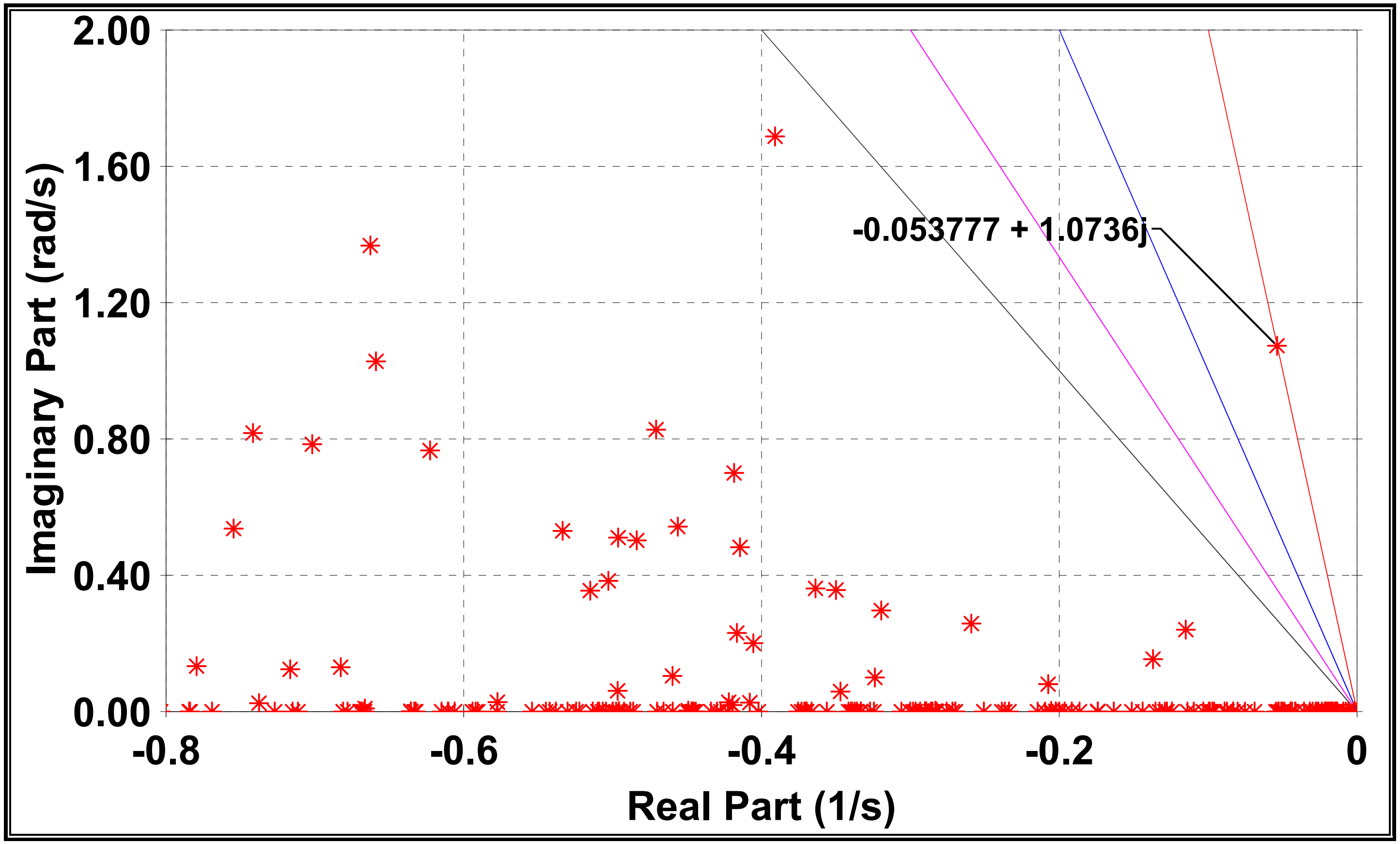

Enlarged View of Small Window in the 1676-Pole Spectrum, for $K_{max} = 2.1172$

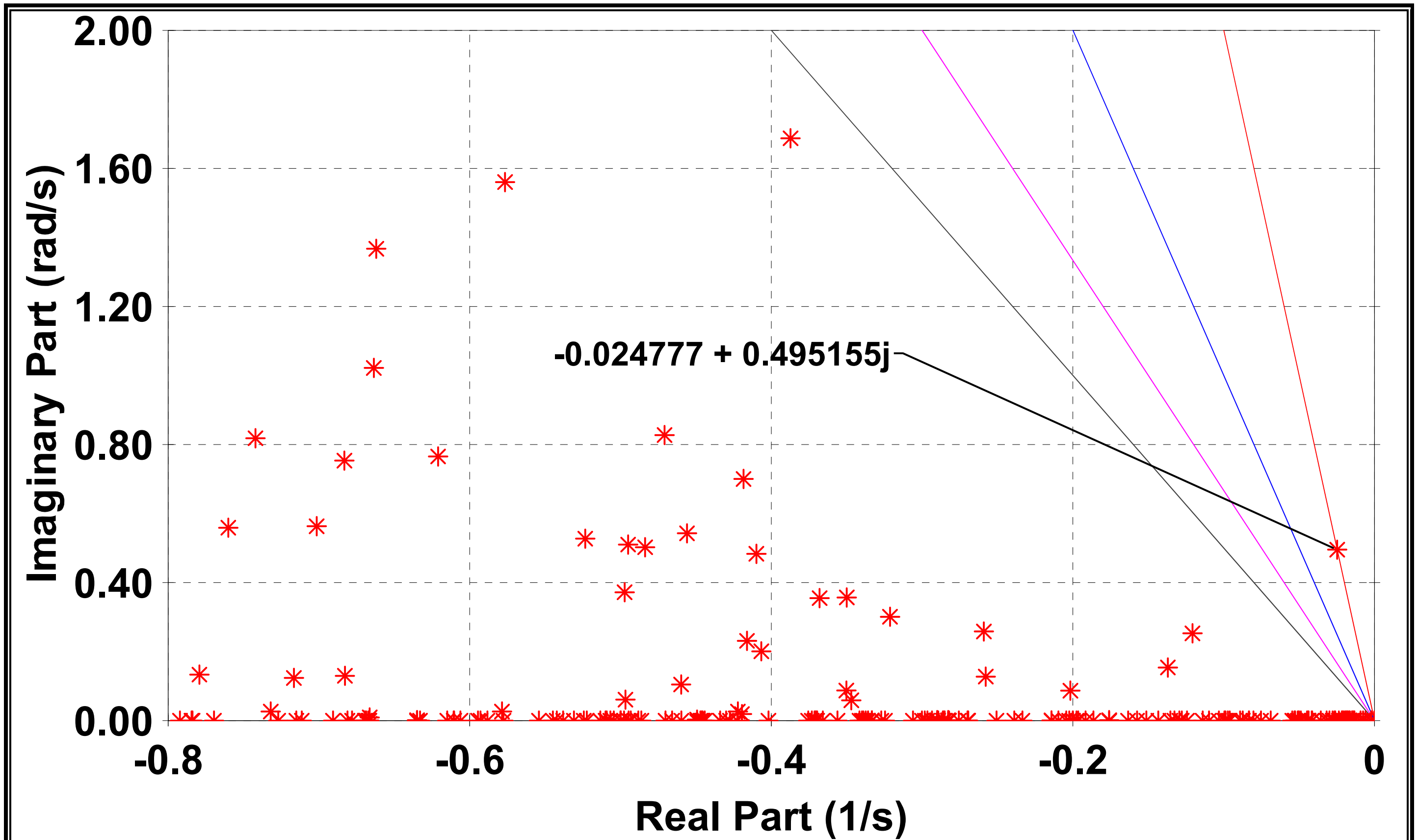

Conclusions

- Developed Hopf algorithm showed robust performance for large-scale systems
- Ensuring that all crossings of the security border have been determined is not an easy task for large-scale problems
- Finding the closest bifurcation point in the multi-parameter space requires optimization techniques (Minimum Distance to Hopf)
- Hopf algorithms and Minimum Distance to Hopf algorithms may be useful in the design of decentralized, non-linear controllers in power systems
- The authors have also been applying these algorithms to other problem areas.